R. & M. No. 3597

R. & M. No. 3597

MINISTRY OF TECHNOLOGY

AERONAUTICAL RESEARCH COUNCIL
REPORTS AND MEMORANDA

Comparison of Three Methods for the Evaluation of Subsonic Lifting-Surface Theory

By H. C. Garner, B. L. Hewitt and T. E. Labrujere

LONDON: HER MAJESTY'S STATIONERY OFFICE
1969
PRICE 19s. 0d. NET

Comparison of Three Methods for the Evaluation of Subsonic Lifting-Surface Theory

By H. C. Garner*, B. L. Hewitt** and T. E. Labrujere***

Reports and Memoranda No. 3597†
June, 1968

Summary

Independent numerical methods for obtaining the subsonic load distribution on a thin wing of arbitrary twist and camber have been developed at NPL, NLR (Netherlands) and BAC (Warton). The three methods have been studied jointly and their novel features have been reviewed critically. The best solutions by each method show excellent agreement for wings, at uniform incidence, having smooth leading and trailing edges. Spanwise loading, local aerodynamic centres, lift, pitching moment, vortex drag and chordwise loadings are tabulated for circular and rectangular planforms, for a wing of constant chord with hyperbolic leading and trailing edges, and for a tapered sweptback wing. The convergence of the solutions is examined in detail with respect to separate parameters representing the numbers of spanwise integration points and spanwise and chordwise collocation points. The tapered sweptback planform is considered with different amounts and types of artificial central rounding, but the crucial problem of a central kink under lifting conditions remains a subject for research.

CONTENTS

*National Physical Laboratory, Teddington.
**British Aircraft Corporation, Warton Aerodrome, Preston.
***National Aerospace Laboratory (NLR), Netherlands.
The names of the authors appear in alphabetical order.
†Replaces NPL Aero Report 1272—A.R.C. 30324.

---

1. *Introduction*

Since the discovery of the possibility under certain circumstances of serious numerical errors in the standard form of Multhopp's subsonic lifting-surface theory (Refs. 1, 2), methods have been developed at NPL, NLR and BAC (Warton) with a view to remedying this situation. In order to get an insight into the qualities of each of the methods, comparative calculations have been made for four different wings (Fig. 1):

(a) the circular planform of aspect ratio $A = 4/\pi$,

(b) the rectangular planform of aspect ratio $A = 2$,

(c) a swept planform of constant chord, having $A = 4$ and hyperbolic leading and trailing edges defined by

$$\left.\begin{aligned} x_l &= \tfrac{3}{4}(1 + 2y^2)^{\frac{1}{2}} - \tfrac{3}{4} \\ x_t &= \tfrac{3}{4}(1 + 2y^2)^{\frac{1}{2}} + \tfrac{1}{4} \end{aligned}\right\} \quad 0 \leqslant |y| \leqslant s = 2, \tag{1}$$

(d) the Warren 12 planform of aspect ratio $2\sqrt{2}$ defined by

$$\left.\begin{aligned} x_l &= (1 + \tfrac{1}{4}\sqrt{2})|y| \\ x_t &= (1 - \tfrac{1}{4}\sqrt{2})|y| + \tfrac{3}{2} \end{aligned}\right\} \quad 0 \leqslant |y| \leqslant s = \sqrt{2}. \tag{2}$$

Each of these wings has been considered at uniform incidence and $M = 0$. The effect of compressibility has not been included in the calculations, as it is covered by the usual factor $\beta = (1 - M^2)^{\frac{1}{2}}$ applied to the spanwise dimensions.

This Report presents the basic theoretical equations and describes the special features of the methods, each of which is formulated to treat smooth planforms. However, BAC plan to modify their basic method in such a way that solutions obtained for kinked planforms would lead to vortex lines that are curved across each kinked section. The rounding of kinks may be achieved in several ways, and it so happens that all three methods would normally use different roundings. However, the NPL and NLR methods are compared for the Warren 12 planform with identical roundings, and the influence of the rounding is examined. The results are discussed relative to the special features of each method and the rate of convergence that is obtained.

2. *Basic Theory*

The fundamental integral equation of subsonic lifting-surface theory may be written in the form

$$\alpha(x, y) = -\frac{1}{8\pi} \fint_{-s}^{s} \frac{dy'}{(y-y')^2} \int_{x_l}^{x_t} \Delta C_p(x', y') \left[1 + \frac{x - x'}{\{(x-x')^2 + \beta^2(y-y')^2\}^{\frac{1}{2}}}\right] dx', \tag{3}$$

where α is a given local incidence and ΔC_p is the unknown load distribution; the double integral is taken over the planform and the bar through the integral sign denotes the principal value according to Mangler in Appendix I of Ref. 1. The unknown loading function is usually approximated by means of an expression

$$\Delta C_p(\xi', \eta') = \frac{4s}{c(\eta')} \sum_{r=0}^{N-1} a_r(\eta') h_r(X'), \tag{4}$$

where

$$h_r(X') = \frac{2}{\pi} \frac{\cos \frac{1}{2}(2r+1)\psi'}{\sin \frac{1}{2}\psi'} \tag{5}$$

and the dimensionless quantities

$$\left.\begin{aligned} \xi' &= x'/s, \qquad \eta' = y'/s \\ X' &= (x' - x_l)/c = \tfrac{1}{2}(1 - \cos \psi') \end{aligned}\right\} \tag{6}$$

are used. The unknown coefficients in their turn may be represented by a trigonometrical polynomial

$$a_r(\eta') = \frac{2}{m+1} \sum_{n=1}^{m} a_{rn} \sum_{\mu=1}^{m} \sin \mu\theta' \sin \frac{\mu n \pi}{m+1} \tag{7}$$

where $\theta' = \cos^{-1}(\eta')$, or by some equivalent power series. Thus the unknown $\Delta C_p(\xi', \eta')$ in equation (3) is replaced by the mN unknown coefficients a_{rn}. The problem is then to calculate a_{rn} by satisfying the boundary condition (3) at suitable pivotal points (x, y) distributed over the planform. The main numerical difficulty lies in determining the double integral due to each term in the representative loading.

In the NPL[3] and NLR[4] methods initial integrations are carried out in the chordwise direction with respect to ξ', and the expression for local incidence becomes

$$\alpha(\xi, \eta) = -\frac{1}{2\pi} \sum_{r=0}^{N-1} \fint_{-1}^{1} \frac{a_r(\eta') H_r(\xi, \eta; \eta')}{(\eta - \eta')^2} d\eta'. \tag{8}$$

It can be shown that this integrand contains the logarithmic singularity

$$-\left(\frac{\beta s}{c(\eta)}\right)^2 a_r(\eta) \log_e|\eta - \eta'| \left(\frac{dh_r}{dX'}\right)_{\eta'=\eta}, \tag{9}$$

which is always removed before the numerical integration in the spanwise direction is attempted. Introduction of the function

$$F_r(\xi, \eta; \eta') = H_r(\xi, \eta; \eta') + \left(\frac{\beta s}{c(\eta)}\right)^2 \left(\frac{dh_r}{dX'}\right)_{\eta'=\eta} (\eta - \eta')^2 \log_e|\eta - \eta'| \tag{10}$$

leads to the integrand

$$\frac{a_r(\eta') F_r(\xi, \eta; \eta')}{(\eta - \eta')^2}, \tag{11}$$

which in the NPL method is treated on the basis of Ref. 2. As is shown in Ref. 4, this integrand is still irregular, because the derivative of F_r with respect to η' does not vanish for $\eta = \eta'$. Therefore within the

NLR method there is introduced the function

$$\bar{H}_r(\xi, \eta; \eta') = \frac{F_r(\xi, \eta; \eta') - F_r(\xi, \eta; \eta) - (\eta - \eta')(\partial F_r/\partial \eta')_{\eta=\eta'}}{(\eta - \eta')^2}, \tag{12}$$

whereby the remaining singularities of the integrand (11) are removed. Since this function is bounded, Fourier analysis is very well suited to perform the integration in spite of the irregularities of the derivatives.

By contrast, in the BAC[5] method initial integrations are carried out along constant percentage chord lines (X' = constant) with respect to η'. Equations (4) to (7) are rewritten in terms of Tchebychev polynomials with coefficients $k_{\rho\nu}$, say. The two terms in the square bracket of equation (3) are treated separately, so that

$$\begin{aligned}\alpha(\xi, \eta) = &-\frac{1}{8\pi}\int_0^1 \int_{-1}^{1} \frac{c(\eta')}{s} \frac{\Delta C_p(\xi', \eta')}{(\eta - \eta')^2} d\eta' \, dX' \\ &+ \frac{1}{8\pi} \sum_{\rho=0}^{N-1} \sum_{\nu=1}^{m} k_{\rho\nu} \int_0^1 T_\rho(X') L_\nu(\xi, \eta; X') \left(\frac{1 - X'}{X'}\right)^{\frac{1}{2}} \frac{dX'}{X' - X},\end{aligned} \tag{13}$$

where $T_\rho(X')$ is a Tchebychev polynomial. The function $L_\nu(\xi, \eta; X')$ results from the initial integration involving the second term in the square bracket, and it can be shown that

$$L_\nu(\xi, \eta; X') = \bar{L}_\nu(\xi, \eta; X') + \sum_{i=1}^{t} K_{\nu i}(X' - X)^i \log_e|X' - X|, \tag{14}$$

where $\bar{L}_\nu(\xi, \eta; X')$ is numerically regular in the range $0 \leqslant X' \leqslant 1$; there may, however, be some restrictions on the range of regularity if η approaches too close to unity. The essential achievement is that from equations (13) and (14) $\alpha(\xi, \eta)$ may be evaluated on the leading and trailing edges.

3. *Description of the Methods*

The NPL, NLR and BAC methods have all been developed to overcome the difficulties which arise when Multhopp's[1] method is applied to the integral equation (3). The special new features of the respective methods will be described briefly.

3.1. *The NPL Method*

In Ref. 3 special attention is given to the chordwise integrals, in order to ensure accurate integration when the number of terms in the pressure series of equation (4) is increased. The accuracy of the spanwise integrals has been made independent of the number of collocation sections in the following manner.

The spanwise integration is performed formally by applying Multhopp's integration scheme with $\bar{m}$ spanwise stations to the integral of equation (8) after removal of the logarithmic singularity (9) in accord with Ref. 2. The expression thus obtained contains $\bar{m}$ unknown values of $a_r(\eta')$ which could be determined from a linear system of equations by satisfying the boundary conditions at $\bar{m}$ spanwise stations. Instead of doing this, Multhopp's interpolation polynomial (7) is applied to each $a_r(\eta')$ to decrease the number of unknowns to the m quantities a_{rn} for each r. Thus the number of spanwise integration points $\bar{m}$ is allowed to exceed the number m of sections where the boundary conditions are to be satisfied, and these are related by the quantity

$$q = (\bar{m} + 1)/(m + 1) \tag{15}$$

which may be unity or any even integer.

The NPL method is programmed in Algol, and a typical running time on the KDF9 computer is 28 minutes when $m = 15$, $N = 4$ and $q = 8$.

3.2. *The NLR Method*

In this method (Ref. 4), special attention has again been paid to the chordwise integration. Sufficient accuracy is guaranteed by adapting the integration scheme to the requirements made by the higher order terms of equations (4) and (5). Detailed analysis of the computing process has achieved remarkable economy in computing time.

Special care has been taken to ensure an accurate spanwise integration. First of all the spanwise integrand has been treated by introducing the function $\bar{H}_r$ of equation (12). Further, the spanwise integration has again been made independent of the number of collocation sections, but differently from the NPL method. In the NLR method first the functions $a_r(\eta')$ are represented by equation (7) with m coefficients a_{rn} for each value of r and then the integration is performed with $\bar{m}$ spanwise stations, whereas in the NPL method the whole numerator of the integrand (11) is represented by means of equation (7). The numbers $\bar{m}$ and m are again related by equation (15), but q can be any positive integer.

The NLR method is programmed in Algol, and a typical running time on the CDC 3300 computer is 22 minutes when $m = 15$, $N = 4$ and $q = 8$.

3.3. *The BAC Method*

As shown in Ref. 5, the basic chordwise integral H_r exhibits an irregular behaviour at $\eta' = \eta$, especially as X tends to zero. A common feature of Refs. 2 to 4 is that the main logarithmic-singularity term (9) is removed for the whole range $-1 \leqslant \eta' \leqslant 1$. This results in the coefficient of the $(\eta - \eta')^2 \log|\eta - \eta'|$ term in equation (10) tending to infinity like $X^{-\frac{3}{2}}$ and $(1 - X)^{-\frac{1}{2}}$ respectively for collocation points near the leading and trailing edges. Elliptic integral analysis has indicated that the irregularity in H_r is not solely associated with the $(\eta - \eta')^2 \log|\eta - \eta'|$ content, which has been proved in Ref. 4, and moreover, that the valid range of η' for its removal tends to zero as X tends to zero or unity.

Therefore BAC[5] have chosen to evaluate the double integral in equation (3) quite differently by carrying out the initial integrations with respect to η' at constant X'. The co-ordinates X' and η' then form a natural and convenient system. Analytical extraction of the $(\eta' - \eta)^{-2}$ content of the integrand is effected, and in evaluating the resulting integral it is found to be advantageous to introduce a particular 'sinh transformation' that stretches the η' scale in the neighbourhood of $\eta' = \eta$. The planform is divided into three basic regions, one containing the section $\eta' = \eta$ where the transformation is applied, and two outer regions covering the residual planform area. Gaussian quadrature techniques are applied to the integrals and give a numerical definition of the function L_ν. The coefficients $K_{\nu i}(\xi, \eta)$, defining the logarithmic singularity in equation (14), are derived analytically and the valid range of X' is only limited if η approaches unity too closely. The modified function $\bar{L}_\nu$ is regular in value and in its first $(t - 1)$ derivatives with respect to X', where arbitrarily $t = 3$. Pseudo-Gaussian quadrature techniques are used to evaluate the principal values of the integrals with respect to X' in equation (13) and hence to provide linear equations relating the unknown coefficients $k_{p\nu}$ to the incidence $\alpha(\xi, \eta)$. The above procedures disconnect the loading function from the integration procedure, so that collocation points can be chosen at will.

The BAC method is programmed in Fortran IV, and a typical running time on the IBM 360/50 computer is $12\frac{1}{2}$ minutes when $m = 15$ and $N = 4$.

4. *Some Critical Remarks on the Different Methods*

The NPL method may be regarded as a step to improve the numerical evaluation of the lifting-surface integral equation. This method shows improved convergence, but it is not completely satisfying in this respect, especially for wings of high aspect ratio or high sweepback. Two causes are suggested, namely, the irregularity of the function F_r and a slight inconsistency in representing both $a_r(\eta')$ and $a_r(\eta')F_r(\xi, \eta; \eta')$ by means of the trigonometrical polynomial (7); the latter implies two different representations of $a_r(\eta)$ at a time. These particular inconsistencies are avoided in the NLR method and, moreover, the infinite singularity of the spanwise integrand has been removed by introducing the function $\bar{H}_r$.

The reasons given in Section 3.3 for BAC's lack of conformity in attacking the lifting-surface problem suggest that the NPL and NLR methods may encounter difficulties when N is large, i.e., when the chordwise collocation points extend close to the leading and trailing edges. This may be generally true of the NPL method, but will not arise since the restriction $N \leqslant 4$ is imposed by the capacity of the KDF9 computer. In practice the NLR method has not suffered from these inferred difficulties. Both NPL and NLR have found that the value of q required to attain convergence of the spanwise integration increases as N increases. In the NPL method this is attributed primarily to the difficulties at the collocation points closest to the leading edge, but from experience at NLR it is suggested that the less smooth behaviour of the higher order terms h_r in the chordwise loading may be a contributory factor. Neither method experiences convergence problems in spanwise integration as m is increased. BAC use a parameter n' to specify the quadrature order when evaluating the integrals involving $\bar{L}_v(X')$ and find that an increase in N has very little effect on the value of n' needed to attain quadrature convergence. For the collocation sections nearest to the tip when $m > 17$, say, significant increases in n' are required in order to maintain quadrature convergence, but this effect has been investigated and can be met by appropriate changes to the BAC programme. While the numerical results from the NPL and NLR methods show the effect of the controlling parameter q, there are no results to demonstrate convergence with respect to n' in the BAC method, and thus the comparisons in Section 5 are especially desirable.

All the methods are at present restricted to planforms with smooth leading and trailing edges. Three separate procedures are suggested for rounding the central kink of a swept wing. Within the NPL method, for wings with straight edges the following formulae for the rounding are usually applied to the leading edge and chord respectively over the range $|y| \leqslant y_i$:

$$\left.\begin{aligned} x_l(y) &= x_l(y_i)[\lambda + \tfrac{1}{6}(1-\lambda)^6] \\ c(y) &= c_R + [\lambda + \tfrac{1}{6}(1-\lambda)^6]\{c(y_i) - c_R\} \end{aligned}\right\}, \tag{16}$$

where $\lambda = |y|/y_i$ and $y_i = s\sin[\pi/(m+1)]$. The corresponding formulae within the NLR method are

$$\left.\begin{aligned} x_l(y) &= x_l(y_i)[\tfrac{1}{3} + \lambda^2 - \tfrac{1}{3}\lambda^3] \\ c(y) &= c_R + [\tfrac{1}{3} + \lambda^2 - \tfrac{1}{3}\lambda^3]\{c(y_i) - c_R\} \end{aligned}\right\}, \tag{17}$$

where the value of y_i is arbitrary. Within the BAC method the corresponding rounding is

$$\left.\begin{aligned} x_l(y) &= x_l(y_i)[\tfrac{5}{16} + \tfrac{15}{16}\lambda^2 - \tfrac{5}{16}\lambda^4 + \tfrac{1}{16}\lambda^6] \\ c(y) &= c_R + [\tfrac{5}{16} + \tfrac{15}{16}\lambda^2 - \tfrac{5}{16}\lambda^4 + \tfrac{1}{16}\lambda^6]\{c(y_i) - c_R\} \end{aligned}\right\}. \tag{18}$$

The roundings give different degrees of regularity in the modified planforms at $y = y_i$ and $y = 0$. The following Table lists the order up to which the y-derivatives of x_l exist at these points.

Rounding	$y = y_i$	$y = 0$
NPL	5th	2nd
NLR	2nd	2nd
BAC	3rd	All

From the definitions in equations (16), (17) and (18) it follows that

$$\left.\begin{aligned} x_l(0)_{\mathrm{NPL}} &= \tfrac{1}{6}x_l(y_i) \quad \text{and} \quad c(0)_{\mathrm{NPL}} = \tfrac{5}{6}c_R + \tfrac{1}{6}c(y_i) \\ x_l(0)_{\mathrm{NLR}} &= \tfrac{1}{3}x_l(y_i) \quad \text{and} \quad c(0)_{\mathrm{NLR}} = \tfrac{2}{3}c_R + \tfrac{1}{3}c(y_i) \\ x_l(0)_{\mathrm{BAC}} &= \tfrac{5}{16}x_l(y_i) \quad \text{and} \quad c(0)_{\mathrm{BAC}} = \tfrac{11}{16}c_R + \tfrac{5}{16}c(y_i) \end{aligned}\right\}. \tag{19}$$

Thus, to give the same displaced root chord as the NPL rounding, the NLR and BAC methods require smaller values of y_i, respectively

$$(y_i)_{\mathrm{NLR}} = \tfrac{1}{2}(y_i)_{\mathrm{NPL}} \quad \text{and} \quad (y_i)_{\mathrm{BAC}} = \tfrac{8}{15}(y_i)_{\mathrm{NPL}}. \tag{20}$$

However, it will be found unsatisfactory to check solutions by the three methods with respective roundings to give identical displacements $x_l(0)$. The local radius of curvature of the rounded leading edge, R, also influences the chordwise loading, and respectively

$$\left.\begin{aligned} R_{\mathrm{NPL}} &= 1{\cdot}200x_l(0)\cot^2\Lambda_l \\ R_{\mathrm{NLR}} &= 1{\cdot}500x_l(0)\cot^2\Lambda_l \\ R_{\mathrm{BAC}} &= 1{\cdot}706x_l(0)\cot^2\Lambda_l \end{aligned}\right\}, \tag{21}$$

where Λ_l is the true angle of leading-edge sweepback.

5. *Discussion of the Results*

As mentioned in the Introduction, the four planforms, (a) circular, (b) rectangular, (c) 'hyperbolic' and (d) 'Warren 12', have been treated as examples (Fig. 1). In the case of the circular wing the overall values of the aerodynamic quantities C_L, C_m and X_{ac} have been compared with the exact values determined by Van Spiegel[6]. No such exact theory is available in the other examples.

Since the Warren 12 planform is kinked at the centre section, some rounding is required. The standard NPL solutions use equation (16) with $m = 15$, but the NPL method can accept arbitrary planform data. The NLR method normally uses equation (17) with $y_i = 0{\cdot}19509s$ giving $x_l(0) = 0{\cdot}08802s$, and in order to obtain fair comparisons between the two methods, both have been applied to this latter rounding and also to that of equation (17) with $y_i = 0{\cdot}09739s$ and $x_l(0) = 0{\cdot}04394s$. For each of these roundings the NLR results for $m = 31$, $N = 4$ and $q = 8$ have been added, because according to Ref. 4 these solutions can be considered to be correct to 3 or 4 figures.

The BAC method cannot yet be applied to the circular tip, but otherwise all three methods have been used. In the following sections the four wings will be discussed one at a time by analysing the solutions obtained and the speed of convergence of the calculations with respect to the various parameters.

5.1. *The Circular Planform*

From Table 1, which presents the NPL solution for $m = 11$, $N = 4$ and $q = 8$ and the NLR solution for $m = 11$, $N = 4$ and $q = 10$, it appears that nearly all the quantities agree to 3 or 4 significant figures with the one exception of the local aerodynamic centre x_{ac} at $\eta = 0{\cdot}9659$. The correctness of the overall aerodynamic quantities can be inferred from the excellent comparisons with the exact values from Ref. 6.

The convergence of the NPL and NLR results can be judged with the help of Table 2 where the variation of x_{ac} with respect to q, m and N is shown. It appears that both methods ensure an equally good convergence with respect to m and N, but that the convergence with respect to q of the NPL results is somewhat slower in the tip region. This explains the aforementioned discrepancy in x_{ac}, which is attributable to the large local sweepback of the leading edge and the improvement in the NLR method associated with equation (12).

5.2. *The Rectangular Planform*

There have been extensive calculations by the BAC method for the rectangular wing of aspect ratio 2. The first part of Table 3 includes results for $m = 7$, 9 and 13, showing rapid convergence with respect to the number of collocation sections. Throughout Table 3 there is perfect agreement between the NLR and BAC solutions with $N = 4$ chordwise terms, and the trivial discrepancies in $\Delta C_p/\alpha$ from the NPL and NLR methods with $m = 15$ and $q = 8$ show that convergence with respect to q is virtually complete. In Table 4, which gives BAC solutions for $m = 13$ and $N = 4$, 5 and 6, results near the tip are slow to converge with respect to N. While the values of $\Delta C_p/\alpha$ at $\eta = 0$, $0{\cdot}3827$ and $0{\cdot}7071$ appear to be correct to about 0·1 per cent when $N = 6$, this is far from true at $\eta = 0{\cdot}9239$. Indeed calculations at this section by the BAC method with smaller m and more chordwise terms suggest that at least $N = 10$ is necessary to achieve such high accuracy.

Evaluation of the leading-edge suction, associated with the singularity in ΔC_p, poses a severe numerical requirement of lifting-surface theory (Ref. 7). The spanwise distribution of vortex drag $cC_{DL}/\bar{c}C_L^2$ from equation (6) of Ref. 7 is slow to converge in Table 4. A searching check on any solution is to compute the vortex drag factor

$$K = \pi A C_{DV}/C_L^2 \tag{22}$$

from surface pressures (K_s) by equation (8) of Ref. 7 and from the wake integral (K_w) by equation (9) of Ref. 7 relating the vortex drag to the cross-flow energy in the wake. The accuracy of $K_w(= 1{\cdot}001)$ is beyond question, and the behaviour of K_s with increasing N, tabulated in Fig. 2, shows convergence within about 0·1 per cent when $N \geqslant 8$. The plotted spanwise distributions of vortex drag do not become indistinguishable near the tip until eight or more chordwise terms are taken.

5.3. *The Hyperbolic Planform*

From Table 5, which presents the comparison of results obtained by NPL, NLR and BAC for $m = 15$, $N = 4$ and $q = 8$ where relevant, it appears that all three methods agree very well. The largest discrepancies occur in the values of $\Delta C_p/\alpha$ for small values of X at $\eta = 0{\cdot}3827$, and here the NLR and BAC results differ by less than 0·1 per cent, both sets differing from the NPL results by about 0·2 per cent.

The deviations between the NPL and NLR results may be explained through the different rates of convergence of ΔC_p with respect to q in Table 6. This convergence can be examined by means of Table 7 which shows the differences

$$\left.\begin{aligned} \delta_3 &= \left(\frac{\Delta C_p}{\alpha}\right)_{q=6} - \left(\frac{\Delta C_p}{\alpha}\right)_{q=4} \\ \delta_4 &= \left(\frac{\Delta C_p}{\alpha}\right)_{q=8} - \left(\frac{\Delta C_p}{\alpha}\right)_{q=6} \end{aligned}\right\}. \tag{23}$$

It appears that the NPL results converge somewhat more slowly than the NLR results. In each case the largest δ_4 occurs near the leading edge at $\eta = 0{\cdot}3827$, where at $X = 0{\cdot}005$ the NPL value is $-0{\cdot}3$ per cent of $\Delta C_p/\alpha$ while the corresponding difference in the NLR results is only a quarter of this.

In Table 8 the convergence of $\Delta C_p/\alpha$ at $\eta = 0{\cdot}3827$ with respect to N is found to be equally good for all three methods, the increments

$$\left.\begin{aligned} \Delta_1 &= \left(\frac{\Delta C_p}{\alpha}\right)_{N=3} - \left(\frac{\Delta C_p}{\alpha}\right)_{N=2} \\ \Delta_2 &= \left(\frac{\Delta C_p}{\alpha}\right)_{N=4} - \left(\frac{\Delta C_p}{\alpha}\right)_{N=3} \end{aligned}\right\} \tag{24}$$

being similar in each case. Table 9 shows the chordwise loading at $\eta = 0{\cdot}3827$ from NLR calculations with $m = 15$, 31 and $N = 3$, 4 and from BAC calculations with $m = 9$, 13, 15 and $N = 4$. Comparison of these results yields the conclusion that at $m = 15$ an accuracy of 3 to 4 figures is obtained. Moreover, it appears that for $m = 15$ and greater the convergence characteristics associated with m are disconnected from those associated with N.

From the foregoing it will be clear that the minor discrepancies in ΔC_p between the NPL results on the one hand, and those from NLR and BAC on the other, are mainly due to the slower convergence of the NPL results with respect to q. For all practical purposes the agreement to about three significant figures is more than adequate.

In Fig. 3 the spanwise distribution of vortex drag has been calculated from equation (6) of Ref. 7. The curves for $N = 2$ and 3 are from the best available solutions by the NPL method, while that for $N = 4$ is from the NLR solution with $m = 31$ and $q = 8$. As in Fig. 2, the results are slowest to converge near the tip, but there is now the complication of negative local drag due to sweepback. The integrated drag factor K_s is again compared with the value $K_w = 1{\cdot}038$ from the wake integral and appears to converge slightly better than for the rectangular wing. The BAC values of K_s for $M = 15$ and $N = 2$, 3 and 4 are identical to those given in Fig. 3.

5.4. *The Warren* 12 *Planform*

Unlike the other three planforms, there is no true solution for the Warren 12 planform based on the loading functions in equations (4) to (7). Although it is planned to develop Ref. 5 to satisfy boundary conditions along the central kink, the present study is limited to planforms with smooth leading and trailing edges. All the calculations correspond roughly to either a small rounding $x_l(0) = 0{\cdot}044s$ or a larger rounding $x_l(0) = 0{\cdot}088s$. For the small rounding and four chordwise terms the spanwise loading, local aerodynamic centres and overall forces from five solutions are given in Table 10. Although they are in broad agreement, the first (NPL) and last (BAC) solutions correspond to respective roundings from equations (16) and (18) and are not strictly comparable with the other three solutions. A precise comparison of the NPL and NLR methods can be made (Section 5), and the two solutions with $m = 15$ for the NLR rounding are found to be the most consistent pair. Their chordwise loadings in the latter part of Table 10 are in very good agreement at $\eta = 0$ and 0·3827; only at $\eta = 0{\cdot}9239$ do the discrepancies occasionally exceed 1 per cent. By contrast, the more accurate NLR results for $m = 31$ exhibit differences of this magnitude at the non-zero values of η, but much larger discrepancies at the centre section. It seems that $m = 15$ gives insufficient collocation sections near the small rounding.

The convergence of the chordwise loadings with respect to q is shown in Table 11. The NPL and NLR methods for $N = 3$, each with its own rounding $x_l(0) = 0{\cdot}044s$, are not expected to converge to the same result as q is increased, but the differences

$$\left.\begin{aligned} \delta_1 &= \left(\frac{\Delta C_p}{\alpha}\right)_{q=2} - \left(\frac{\Delta C_p}{\alpha}\right)_{q=1} \\ \delta_2 &= \left(\frac{\Delta C_p}{\alpha}\right)_{q=4} - \left(\frac{\Delta C_p}{\alpha}\right)_{q=2} \end{aligned}\right\} \tag{25}$$

and δ_3 from equation (23) illustrate the rate of convergence. The superior convergence of the NLR method can be seen in Figs. 4 and 5 for $\eta = 0{\cdot}3827$ and $0{\cdot}9239$ respectively. At the same time the magnitudes of δ_1 in the upper diagrams of Figs. 4 and 5 reveal the serious numerical errors in the earlier standard form of Multhopp's theory equivalent to the NPL method with $q = 1$.

Table 12 presents the results obtained by NPL and NLR for $m = 15$, $N = 4$, $q = 8$ and the larger NLR rounding $x_l(0) = 0{\cdot}088s$. The agreement is quite as good as for the small rounding in Table 10. The new feature is that the more accurate loading from the NLR solution for $m = 31$, $N = 4$ and $q = 8$, which is correct to 3 or 4 figures (Ref. 4), is everywhere practically within 1 per cent of both results for $m = 15$. This suggests that convergence with respect to m is better for the larger rounding.

Convergence with respect to N has been studied for the small rounding by the NPL and NLR methods and for the larger rounding by the BAC method. The former results are presented graphically for $\eta = 0{\cdot}3827$ in Fig. 6, where Δ_1 and Δ_2 from equations (24) show completely similar behaviour from the two methods and roughly $\Delta_2 < \frac{1}{3}\Delta_1$. The solutions for $m = 15$ and $N = 2$, 3 and 4 obtained by BAC are given in Table 13. The convergence is much better at $\eta = 0{\cdot}3827$ and $0{\cdot}7071$ than at $\eta = 0$ and much worse at $\eta = 0{\cdot}9239$. Nevertheless, over the inner part of the span the larger rounding appears to improve the convergence and make less demands on N. Table 13 also includes the spanwise distribution of vortex drag $cC_{DL}/\bar{c}C_L^2$ and the vortex drag factors K_s and K_w (Section 5.2). Whilst the two factors for $N = 4$ are within 1 per cent and agree as well as those for the rectangular and hyperbolic planforms in Figs. 2 and 3, the corresponding values of K_s and K_w in Table 10 for the small rounding differ by 5 per cent; however, both factors in Table 10 from the NLR solution with $m = 31$ show remarkable agreement with those in Table 13 with $m = 15$. This provides further evidence that for expediency of convergence the larger roundings of equations (17) and (18) are preferable to the NPL rounding in equation (16).

In all, with $m = 15$ and $N = 4$, five distinct roundings have been considered, and the central chordwise loadings are collected in Table 14. To eliminate the leading-edge singularity, $(\Delta C_p/\alpha)X^{\frac{1}{2}}$ is plotted against X in Fig. 7. The large effect of the change in the leading-edge displacement $x_l(0)$ is expected, but there is also an appreciable secondary effect of the local radius of curvature from equation (21). These loadings at $\eta = 0$ have no aerodynamic significance for the actual Warren 12 planform, and the results in Tables 10 and 12 indicate that the effects of the rounding are felt over an appreciable part of the span. The guiding principle in choosing the artificial rounding is that it should be the smallest that will not jeopardize the convergence of the solution.

6. *Concluding Remarks*

From the results presented it may be concluded that, for smooth planforms of moderate aspect ratio and for $N \leqslant 4$, all three methods produce consistent numerical results provided that quadrature accuracies are maintained. Fully correct 'aerodynamic' results for ΔC_p would require larger values of N, as is demonstrated for the rectangular planform; for cambered wings the need for a considerable increase in N can be expected, and in this respect the points raised in Sections 3.3 and 4 may discourage the extension of the NPL method to $N > 4$. The NLR method should remain satisfactory for larger values of N if an appropriate value of q is applied. The functioning of the BAC method is shown to be unimpaired as N increases.

It is observed that the NPL results show a slower convergence with respect to the number of spanwise integration points than those of NLR. Obviously, the appearance of a near kink in the planform could aggravate this phenomenon. But it is encouraging that discrepancies between the NPL and NLR results for the smoothed Warren 12 planform remain small when the rounding is reduced from $x_l(0) = 0{\cdot}088s$ to $x_l(0) = 0{\cdot}044s$. The load distributions at $\eta = 0$ are very sensitive to the amount of rounding, and limitations of this artifice are exposed.

In all cases considered, the convergence with respect to N is equally good for the three methods. But, as is shown in Ref. 4, this convergence is strongly dependent on the accuracy of the spanwise integration, especially as the aspect ratio increases above 4, say. Therefore it may be doubted whether the NPL method will exhibit equally good convergence for wings of high aspect ratio owing to capacity restrictions on q.

The convergence with respect to m is excellent for the circular, rectangular and hyperbolic planforms. For the Warren 12 planform, especially with the smaller artificial rounding, it is necessary to take more than 15 collocation sections; even so, the NLR results with $m = 31$ differ primarily at $\eta = 0$ where solutions have little relevance to the actual wing. For the practical objective of obtaining load distributions at adjacent sections it is necessary to compromise between an accurate solution for too large a rounding and one for too small a rounding that has not converged with respect to m.

Finally it is worth mentioning a number of subjects that require further research, e.g., the influence of increasing aspect ratio or decreasing rounding on the rates of convergence with respect to the numbers of spanwise and chordwise collocation points, the accuracy obtainable for the chordwise loading of cambered wings, and the effects of collocation point positioning on the accuracy and stability of solutions. The determination of reliable solutions for kinked planforms remains a crucial problem. However, it may be assumed that the comparisons established in this report have achieved a sufficient appraisal of the three basic methods with respect to each other.

LIST OF SYMBOLS

a_r	Coefficient of h_r, varying in spanwise direction
a_{rn}	Unknown coefficients in equation (7)
A	Aspect ratio; $2s/\bar{c}$
c	Local chord
$\bar{c}$	Geometric mean chord; $S/2s$
c_R	Root chord, without artificial central rounding
C_{DL}	Local drag coefficient; local drag/$\frac{1}{2}\rho U^2 c$
C_{DV}	Vortex drag coefficient; vortex drag/$\frac{1}{2}\rho U^2 S$
C_L	Lift coefficient; lift/$\frac{1}{2}\rho U^2 S$
C_{LL}	Local lift coefficient; local lift/$\frac{1}{2}\rho U^2 c$
C_m	Nose-up pitching moment about root leading edge/$\frac{1}{2}\rho U^2 S\bar{c}$
C_p	Pressure coefficient; ΔC_p = pressure difference/$\frac{1}{2}\rho U^2$
F_r	Function defined in equation (10)
h_r	Chordwise function in equation (5)
H_r	Initial chordwise integral
$\bar{H}_r$	Regularized function defined in equation (12)
$k_{\rho\nu}$	Unknown coefficients in equation (13)

K_s	Vortex drag factor $\pi A C_{DV}/C_L^2$ from surface pressures
K_w	Vortex drag factor $\pi A C_{DV}/C_L^2$ from wake integral
K_{vi}	Coefficients in equation (14) with $i = 1, 2, \ldots t$
L_v	Initial spanwise integral
$\bar{L}_v$	Regularized function defined in equation (14)
m	Number of collocation sections
$\bar{m}$	Number of spanwise integration points; $q(m + 1) - 1$
M	Mach number of undisturbed stream
n'	Parameter specifying numerical integration with respect to X' in equation (13)
N	Number of chordwise functions
q	Factor; $(\bar{m} + 1)/(m + 1)$
r	Index numerating chordwise function
R	Radius of curvature of rounded leading edge at $\eta = 0$
s	Semi-span of wing
S	Area of planform
U	Velocity of undisturbed stream
$\left.\begin{matrix} x, y \\ x', y' \end{matrix}\right\}$	Rectangular co-ordinates referred to root leading-edge
x_{ac}	Local centre of pressure in terms of X
x_l	Ordinate of leading edge
x_t	Ordinate of trailing edge
X, X'	Local chordwise position; $(x - x_l)/c$, $(x' - x_l)/c$
X_{ac}	Centre of pressure referred to $\bar{c}$; $-C_m/C_L$
y_i	Outer limit of artificial central rounding of swept wing
α	Local incidence of wing (radians)
β	Compressibility factor; $(1 - M^2)^{\frac{1}{2}}$
δ_i	Increments in $\Delta C_p/\alpha$ in equations (23) and (25) due to increasing q
Δ_i	Increments in $\Delta C_p/\alpha$ in equations (24) due to increasing N
η, η'	Spanwise ordinate; y/s, y'/s
θ'	Spanwise parameter; $\cos^{-1} \eta'$
Λ_l	Angle of sweepback of leading edge
v	Index numerating spanwise loading function
ξ, ξ'	Streamwise ordinate; x/s, x'/s
ρ	Density of undisturbed stream
ψ'	Chordwise parameter; $\cos^{-1}(1 - 2X')$

REFERENCES

No.	*Author(s)*	*Title, etc.*
1	H. Multhopp	Methods for calculating the lift distribution of wings (Subsonic lifting surface theory). A.R.C. R. & M. 2884. January, 1950.
2	K. W. Mangler and B. F. R. Spencer	Some remarks on Multhopp's subsonic lifting-surface theory. A.R.C. R. & M. 2926. August, 1952.
3	H. C. Garner and D. A. Fox ..	Algol 60 programme for Multhopp's low-frequency subsonic lifting-surface theory. A.R.C. R. & M. 3517. April, 1966.
4	P. J. Zandbergen, T. E. Labrujere and J. G. Wouters	A new approach to the numerical solution of the equation of subsonic lifting surface theory. N.L.R. Report TR G.49. November, 1967.
5	B. L. Hewitt	Developments in subsonic lifting surface theory. B.A.C. Preston Division Report Ae 282. A.R.C. Report 29 488. September, 1967.
6	E. van Spiegel	Boundary value problems in lifting surface theory. Thesis T.H. Delft. February, 1959. N.L.L. Tech. Report W.1. March, 1959.
7	H. C. Garner	Some remarks on vortex drag and its spanwise distribution in incompressible flow. Aeronaut. J. (R. Ae. S.) Tech. Note. July, 1968.

TABLE 1

Results for the Circular Planform ($M = 0, m = 11, N = 4$).

η	Values of $cC_{LL}/\bar{c}C_L$		Values of x_{ac}	
	NPL $q = 8$	NLR $q = 10$	NPL $q = 8$	NLR $q = 10$
0	1·2844	1·2844	0·1980	0·1980
0·2588	1·2387	1·2386	0·1970	0·1970
0·5000	1·1049	1·1049	0·1938	0·1938
0·7071	0·8937	0·8937	0·1876	0·1877
0·8660	0·6219	0·6220	0·1764	0·1768
0·9659	0·3138	0·3139	0·1551	0·1578

	Overall values		
	NPL $q = 8$	NLR $q = 10$	Exact Ref. 6
C_L	1·7903	1·7903	1·7902
$-C_m$	0·5459	0·5461	0·5460
X_{ac}	0·3049	0·3050	0·3050

X	$\Delta C_p/\alpha$ at $\eta = 0$		$\Delta C_p/\alpha$ at $\eta = 0{\cdot}5$		$\Delta C_p/\alpha$ at $\eta = 0{\cdot}866$	
	NPL ($q = 8$)	NLR ($q = 10$)	NPL ($q = 8$)	NLR ($q = 10$)	NPL ($q = 8$)	NLR ($q = 10$)
0·0050	19·481	19·480	19·591	19·591	20·040	20·026
0·0125	12·220	12·220	12·292	12·292	12·586	12·577
0·0250	8·522	8·522	8·575	8·575	8·790	8·784
0·05	5·856	5·856	5·894	5·894	6·050	6·046
0·10	3·898	3·898	3·921	3·920	4·017	4·014
0·15	2·982	2·982	2·993	2·993	3·043	3·041
0·20	2·408	2·408	2·409	2·408	2·417	2·416
0·30	1·684	1·684	1·667	1·667	1·602	1·603
0·40	1·223	1·223	1·192	1·193	1·075	1·077
0·50	0·896	0·896	0·858	0·859	0·713	0·715
0·60	0·651	0·651	0·614	0·614	0·467	0·469
0·70	0·464	0·464	0·432	0·432	0·308	0·310
0·80	0·315	0·316	0·295	0·295	0·213	0·215
0·90	0·190	0·190	0·182	0·182	0·153	0·154
0·95	0·125	0·125	0·123	0·123	0·116	0·117

TABLE 2

Convergence of x_{ac} for the Circular Planform ($M = 0$)

(a) Effect of q

η	NPL method ($m = 11$, $N = 4$)			NLR method ($m = 11$, $N = 4$)		
	$q = 4$	$q = 6$	$q = 8$	$q = 6$	$q = 8$	$q = 10$
0	0·1981	0·1980	0·1980	0·1980	0·1980	0·1980
0·2588	0·1971	0·1970	0·1970	0·1970	0·1970	0·1970
0·5000	0·1939	0·1938	0·1938	0·1938	0·1938	0·1938
0·7071	0·1879	0·1876	0·1876	0·1877	0·1877	0·1877
0·8660	0·1783	0·1769	0·1764	0·1768	0·1768	0·1768
0·9659	0·1702	0·1597	0·1551	0·1573	0·1581	0·1578

(b) Effect of N

η	NPL method ($m = 11$)			NLR method ($m = 5$)		
	$N = 2$ $q = 4$	$N = 3$ $q = 6$	$N = 4$ $q = 8$	$N = 2$ $q = 8$	$N = 3$ $q = 8$	$N = 4$ $q = 8$
0	0·1958	0·1981	0·1980	0·1960	0·1982	0·1980
0·2588	0·1945	0·1971	0·1970			
0·5000	0·1904	0·1939	0·1938	0·1905	0·1940	0·1938
0·7071	0·1828	0·1880	0·1876			
0·8660	0·1702	0·1780	0·1764	0·1724	0·1786	0·1768
0·9659	0·1515	0·1603	0·1551			

(c) Effect of m

η	NPL method ($N = 4$)		NLR method ($N = 4$)	
	$m = 5$	$m = 11$	$m = 5$	$m = 11$
0	0·1982	0·1980	0·1980	0·1980
0·2588		0·1970		0·1970
0·5000	0·1938	0·1938	0·1938	0·1938
0·7071		0·1876		0·1877
0·8660	0·1784	0·1764	0·1768	0·1768
0·9659		0·1551		0·1578

TABLE 3

Results for the Rectangular Planform ($M = 0, N = 4, q = 8$)

	NPL $m = 15$	NLR $m = 15$	BAC $m = 7$	BAC $m = 9$	BAC $m = 13$
η	Values of $cC_{LL}/\bar{c}C_L$				
0	1·2543	1·2543	1·2543	1·2543	1·2543
0·1951	1·2331	1·2331	1·2331	1·2331	1·2331
0·3827	1·1692	1·1692	1·1692	1·1692	1·1692
0·5556	1·0625	1·0625	1·0625	1·0625	1·0625
0·7071	0·9137	0·9137	0·9137	0·9137	0·9137
0·8315	0·7257	0·7258	0·7257	0·7257	0·7257
0·9239	0·5044	0·5044	0·5044	0·5044	0·5044
0·9808	0·2587	0·2587	0·2586	0·2586	0·2586
η	Values of x_{ac}				
0	0·2199	0·2199	0·2199	0·2199	0·2199
0·1951	0·2187	0·2187	0·2187	0·2186	0·2187
0·3827	0·2149	0·2149	0·2149	0·2149	0·2149
0·5556	0·2085	0·2085	0·2085	0·2085	0·2085
0·7071	0·1996	0·1996	0·1995	0·1996	0·1996
0·8315	0·1886	0·1886	0·1885	0·1886	0·1886
0·9239	0·1773	0·1773	0·1773	0·1773	0·1773
0·9808	0·1685	0·1685	0·1688	0·1685	0·1685
η	Values of $cC_{DL}/\bar{c}C_L^2$				
0	0·1847	0·1848	0·1847	0·1848	0·1848
0·1951	0·1831	0·1832	0·1831	0·1832	0·1832
0·3827	0·1781	0·1781	0·1782	0·1781	0·1781
0·5556	0·1686	0·1686	0·1691	0·1686	0·1686
0·7071	0·1540	0·1541	0·1540	0·1541	0·1541
0·8315	0·1353	0·1353	0·1347	0·1353	0·1353
0·9239	0·1130	0·1131	0·1131	0·1130	0·1131
0·9808	0·0770	0·0770	0·0773	0·0770	0·0770
	Overall values				
C_L	2·4745	2·4744	2·4744	2·4744	2·4744
$-C_m$	0·5182	0·5182	0·5182	0·5182	0·5182
X_{ac}	0·2094	0·2094	0·2094	0·2094	0·2094
K_s	1·0104	1·0108	1·0107	1·0108	1·0108
K_w	1·0007	1·0007	1·0006	1·0006	1·0006

TABLE 3 (continued)

Results for the Rectangular Planform ($M = 0, N = 4, q = 8$)

X	$\Delta C_p/\alpha$ at $\eta = 0$ NPL $m = 15$	$\Delta C_p/\alpha$ at $\eta = 0$ NLR $m = 15$	$\Delta C_p/\alpha$ at $\eta = 0$ BAC $m = 13$	$\Delta C_p/\alpha$ at $\eta = 0{\cdot}3827$ NPL $m = 15$	$\Delta C_p/\alpha$ at $\eta = 0{\cdot}3827$ NLR $m = 15$	$\Delta C_p/\alpha$ at $\eta = 0{\cdot}3827$ BAC $m = 13$
0·0050	31·530	31·524	31·525	30·117	30·113	30·113
0·0125	19·782	19·779	19·779	18·873	18·871	18·871
0·0250	13·801	13·800	13·800	13·142	13·140	13·141
0·05	9·498	9·497	9·497	9·010	9·009	9·010
0·10	6·355	6·355	6·355	5·985	5·985	5·985
0·15	4·903	4·903	4·903	4·586	4·586	4·586
0·20	4·006	4·006	4·006	3·722	3·722	3·722
0·30	2·895	2·895	2·895	2·660	2·660	2·660
0·40	2·200	2·200	2·200	2·002	2·002	2·002
0·50	1·707	1·707	1·707	1·542	1·542	1·542
0·60	1·329	1·329	1·329	1·194	1·194	1·194
0·70	1·020	1·020	1·020	0·914	0·914	0·914
0·80	0·751	0·750	0·750	0·671	0·671	0·671
0·90	0·485	0·485	0·485	0·434	0·434	0·434
0·95	0·330	0·330	0·330	0·295	0·295	0·295

X	$\Delta C_p/\alpha$ at $\eta = 0{\cdot}7071$ NPL $m = 15$	$\Delta C_p/\alpha$ at $\eta = 0{\cdot}7071$ NLR $m = 15$	$\Delta C_p/\alpha$ at $\eta = 0{\cdot}7071$ BAC $m = 13$	$\Delta C_p/\alpha$ at $\eta = 0{\cdot}9239$ NPL $m = 15$	$\Delta C_p/\alpha$ at $\eta = 0{\cdot}9239$ NLR $m = 15$	$\Delta C_p/\alpha$ at $\eta = 0{\cdot}9239$ BAC $m = 13$
0·0050	25·660	25·659	25·658	16.543	16·540	16·540
0·0125	15·999	15·998	15·998	10·198	10·197	10·197
0·0250	11·047	11·046	11·046	6·911	6·910	6·910
0·05	7·451	7·450	7·450	4·491	4·491	4·490
0·10	4·798	4·798	4·798	2·691	2·690	2·690
0·15	3·574	3·574	3·574	1·874	1·874	1·874
0·20	2·828	2·828	2·828	1·398	1·398	1·398
0·30	1·940	1·940	1·940	0·884	0·883	0·884
0·40	1·421	1·421	1·421	0·632	0·632	0·632
0·50	1·080	1·080	1·080	0·495	0·494	0·494
0·60	0·834	0·834	0·834	0·404	0·404	0·404
0·70	0·640	0·640	0·640	0·327	0·327	0·327
0·80	0·472	0·472	0·472	0·244	0·244	0·244
0·90	0·305	0·305	0·305	0·149	0·149	0·149
0·95	0·206	0·206	0·206	0·093	0·093	0·093

TABLE 4

Convergence of Solutions with Respect to N for the Rectangular Planform ($M = 0, m = 13$)

η	Values of $cC_{LL}/\bar{c}C_L$			Values of x_{ac}		
	BAC method			BAC method		
	$N = 4$	$N = 5$	$N = 6$	$N = 4$	$N = 5$	$N = 6$
0	1·2543	1·2543	1·2543	0·2199	0·2199	0·2199
0·1951	1·2331	1·2330	1·2330	0·2187	0·2187	0·2187
0·3827	1·1692	1·1692	1·1692	0·2149	0·2149	0·2149
0·5556	1·0625	1·0625	1·0625	0·2085	0·2085	0·2085
0·7071	0·9137	0·9137	0·9137	0·1996	0·1996	0·1996
0·8315	0·7257	0·7257	0·7257	0·1886	0·1886	0·1886
0·9239	0·5044	0·5045	0·5044	0·1773	0·1771	0·1770
0·9808	0·2586	0·2587	0·2587	0·1685	0·1679	0·1674

η	Values of $cC_{DL}/\bar{c}C_L^2$		
	BAC method		
	$N = 4$	$N = 5$	$N = 6$
0	0·1848	0·1850	0·1850
0·1951	0·1832	0·1834	0·1835
0·3827	0·1781	0·1785	0·1786
0·5556	0·1686	0·1690	0·1693
0·7071	0·1541	0·1536	0·1539
0·8315	0·1353	0·1320	0·1315
0·9239	0·1131	0·1068	0·1033
0·9808	0·0770	0·0732	0·0701

	Overall values		
	BAC method		
	$N = 4$	$N = 5$	$N = 6$
C_L	2·4744	2·4744	2·4744
$-C_m$	0·5182	0·5181	0·5181
X_{ac}	0·2094	0·2094	0·2094
K_s	1·0108	1·0054	1·0033
K_w	1·0006	1·0007	1·0007

TABLE 4 (continued)

Convergence of Solutions with Respect to N for the Rectangular Planform ($M = 0, m = 13$)

X	Values of $\Delta C_p/\alpha$ at $\eta = 0$			Values of $\Delta C_p/\alpha$ at $\eta = 0{\cdot}3827$		
	BAC method			BAC method		
	$N = 4$	$N = 5$	$N = 6$	$N = 4$	$N = 5$	$N = 6$
0·0050	31·5251	31·5175	31·5171	30·1132	30·0982	30·0956
0·0125	19·7792	19·7760	19·7759	18·8712	18·8646	18·8639
0·0250	13·7998	13·7991	13·7992	13·1408	13·1390	13·1394
0·05	9·4973	9·4986	9·4988	9·0095	9·0113	9·0124
0·10	6·3550	6·3571	6·3573	5·9847	5·9883	5·9891
0·15	4·9030	4·9047	4·9047	4·5856	4·5886	4·5889
0·20	4·0058	4·0067	4·0067	3·7225	3·7243	3·7240
0·30	2·8953	2·8949	2·8948	2·6598	2·6593	2·6587
0·40	2·2004	2·1994	2·1994	2·0022	2·0007	2·0005
0·50	1·7070	1·7063	1·7064	1·5417	1·5406	1·5408
0·60	1·3288	1·3288	1·3289	1·1937	1·1936	1·1939
0·70	1·0202	1·0208	1·0208	0·9136	0·9144	0·9144
0·80	0·7504	0·7510	0·7509	0·6710	0·6719	0·6716
0·90	0·4850	0·4849	0·4849	0·4339	0·4338	0·4336
0·95	0·3296	0·3291	0·3292	0·2951	0·2944	0·2945

X	Values of $\Delta C_p/\alpha$ at $\eta = 0{\cdot}7071$			Values of $\Delta C_p/\alpha$ at $\eta = 0{\cdot}9239$		
	BAC method			BAC method		
	$N = 4$	$N = 5$	$N = 6$	$N = 4$	$N = 5$	$N = 6$
0·0050	25·6585	25·6809	25·6668	16·5395	17·0241	17·2606
0·0125	15·9976	16·0064	16·0010	10·1966	10·4213	10·5097
0·0250	11·0465	11·0472	11·0469	6·9101	6·9840	6·9872
0·05	7·4503	7·4452	7·4482	4·4904	4·4497	4·3966
0·10	4·7980	4·7909	4·7944	2·6904	2·5929	2·5349
0·15	3·5737	3·5686	3·5706	1·8739	1·7871	1·7574
0·20	2·8284	2·8262	2·8266	1·3983	1·3421	1·3404
0·30	1·9400	1·9426	1·9413	0·8835	0·8892	0·9128
0·40	1·4214	1·4255	1·4246	0·6323	0·6677	0·6808
0·50	1·0796	1·0822	1·0823	0·4945	0·5243	0·5177
0·60	0·8335	0·8332	0·8338	0·4041	0·4084	0·3942
0·70	0·6402	0·6377	0·6379	0·3267	0·3074	0·3028
0·80	0·4723	0·4699	0·4694	0·2444	0·2230	0·2320
0·90	0·3049	0·3052	0·3049	0·1487	0·1530	0·1580
0·95	0·2063	0·2082	0·2084	0·0933	0·1131	0·1074

TABLE 5

Results for the Hyperbolic Planform ($M = 0, m = 15, N = 4$)

η	Values of $cC_{LL}/\bar{c}C_L$			Values of x_{ac}		
	NPL $q = 8$	NLR $q = 8$	BAC	NPL $q = 8$	NLR $q = 8$	BAC
0	1·1293	1·1290	1·1291	0·2739	0·2737	0·2738
0·1951	1·1284	1·1283	1·1283	0·2665	0·2663	0·2663
0·3827	1·1192	1·1192	1·1191	0·2545	0·2542	0·2542
0·5556	1·0872	1·0873	1·0872	0·2422	0·2420	0·2420
0·7071	1·0076	1·0078	1·0077	0·2217	0·2216	0·2216
0·8315	0·8512	0·8514	0·8513	0·1843	0·1843	0·1843
0·9239	0·6152	0·6153	0·6153	0·1354	0·1355	0·1354
0·9808	0·3216	0·3217	0·3216	0·0920	0·0920	0·0920

	Overall values		
	NPL $q = 8$	NLR $q = 8$	BAC
C_L	3·2335	3·2327	3·2326
$-C_m$	2·4798	2·4789	2·4788
X_{ac}	0·7669	0·7668	0·7668

TABLE 5 (continued)

Results for the Hyperbolic Planform ($M = 0, m = 15, N = 4$)

X	$\Delta C_p/\alpha$ at $\eta = 0$			$\Delta C_p/\alpha$ at $\eta = 0{\cdot}3827$		
	NPL $q = 8$	NLR $q = 8$	BAC	NPL $q = 8$	NLR $q = 8$	BAC
0·0050	29·791	29·770	29·772	31·643	31·714	31·709
0·0125	18·830	18·818	18·819	19·965	20·006	20·002
0·0250	13·299	13·292	13·293	14·060	14·083	14·081
0·05	9·378	9·375	9·375	9·857	9·867	9·866
0·10	6·584	6·583	6·583	6·840	6·839	6·839
0·15	5·325	5·325	5·325	5·467	5·463	5·463
0·20	4·557	4·558	4·558	4·624	4·618	4·618
0·30	3·606	3·608	3·608	3·570	3·564	3·564
0·40	2·993	2·995	2·994	2·885	2·880	2·880
0·50	2·530	2·531	2·530	2·367	2·364	2·364
0·60	2·141	2·140	2·140	1·936	1·934	1·934
0·70	1·781	1·778	1·779	1·551	1·549	1·549
0·80	1·415	1·410	1·411	1·180	1·178	1·177
0·90	0·983	0·978	0·979	0·781	0·778	0·778
0·95	0·692	0·688	0·688	0·535	0·533	0·532

X	$\Delta C_p/\alpha$ at $\eta = 0{\cdot}7071$			$\Delta C_p/\alpha$ at $\eta = 0{\cdot}9239$		
	NPL $q = 8$	NLR $q = 8$	BAC	NPL $q = 8$	NLR $q = 8$	BAC
0·0050	31·786	31·812	31·807	28·802	28·803	28·800
0·0125	20·013	20·028	20·025	17·799	17·800	17·798
0·0250	14·043	14·051	14·050	12·107	12·109	12·106
0·05	9·771	9·774	9·773	7·915	7·915	7·914
0·10	6·667	6·666	6·666	4·766	4·765	4·765
0·15	5·230	5·228	5·227	3·298	3·297	3·297
0·20	4·331	4·329	4·329	2·409	2·409	2·408
0·30	3·188	3·186	3·186	1·383	1·383	1·382
0·40	2·437	2·435	2·436	0·833	0·833	0·833
0·50	1·878	1·877	1·877	0·520	0·520	0·519
0·60	1·431	1·431	1·431	0·336	0·336	0·336
0·70	1·060	1·060	1·060	0·227	0·227	0·227
0·80	0·740	0·740	0·739	0·157	0·157	0·157
0·90	0·445	0·445	0·445	0·101	0·101	0·101
0·95	0·290	0·290	0·290	0·069	0·069	0·069

TABLE 6

Chordwise Loading of the Hyperbolic Planform ($M = 0, m = 15, N = 4$)

X	$\Delta C_p/\alpha$ at $\eta = 0$					
	NPL method			NLR method		
	$q = 4$	$q = 6$	$q = 8$	$q = 4$	$q = 6$	$q = 8$
0·0050	29·992	29·822	29·791	29·750	29·772	29·770
0·0125	18·946	18·847	18·830	18·806	18·819	18·818
0·0250	13·368	13·309	13·299	13·285	13·293	13·292
0·05	9·411	9·382	9·378	9·371	9·376	9·375
0·10	6·588	6·583	6·584	6·583	6·584	6·583
0·15	5·318	5·322	5·325	5·326	5·327	5·325
0·20	4·545	4·553	4·557	4·560	4·560	4·558
0·30	3·593	3·603	3·606	3·610	3·610	3·608
0·40	2·984	2·991	2·993	2·996	2·996	2·995
0·50	2·525	2·530	2·530	2·531	2·532	2·531
0·60	2·139	2·141	2·141	2·138	2·140	2·140
0·70	1·782	1·782	1·781	1·775	1·778	1·778
0·80	1·415	1·416	1·415	1·406	1·410	1·410
0·90	0·982	0·985	0·983	0·974	0·978	0·978
0·95	0·690	0·693	0·692	0·684	0·687	0·688

X	$\Delta C_p/\alpha$ at $\eta = 0{\cdot}3827$					
	NPL method			NLR method		
	$q = 4$	$q = 6$	$q = 8$	$q = 4$	$q = 6$	$q = 8$
0·0050	31·749	31·531	31·643	31·785	31·740	31·714
0·0125	20·026	19·901	19·965	20·046	20·020	20·006
0·0250	14·096	14·022	14·060	14·107	14·091	14·083
0·05	9·874	9·840	9·857	9·877	9·870	9·867
0·10	6·842	6·838	6·840	6·839	6·839	6·839
0·15	5·463	5·472	5·467	5·459	5·462	5·463
0·20	4·616	4·632	4·624	4·612	4·617	4·618
0·30	3·561	3·578	3·570	3·558	3·565	3·564
0·40	2·879	2·891	2·885	2·875	2·883	2·880
0·50	2·365	2·371	2·367	2·361	2·369	2·364
0·60	1·940	1·940	1·936	1·932	1·940	1·934
0·70	1·558	1·554	1·551	1·547	1·555	1·549
0·80	1·191	1·184	1·180	1·175	1·182	1·178
0·90	0·793	0·786	0·781	0·776	0·781	0·778
0·95	0·544	0·540	0·535	0·530	0·533	0·533

TABLE 6 (continued)

Chordwise Loading of the Hyperbolic Planform ($M = 0, m = 15, N = 4$)

X	$\Delta C_p/\alpha$ at $\eta = 0{\cdot}7071$					
	NPL method			NLR method		
	$q = 4$	$q = 6$	$q = 8$	$q = 4$	$q = 6$	$q = 8$
0·0050	31·527	31·682	31·786	31·838	31·823	31·812
0·0125	19·867	19·955	20·013	20·043	20·038	20·028
0·0250	13·959	14·010	14·043	14·060	14·060	14·051
0·05	9·735	9·757	9·771	9·777	9·784	9·774
0·10	6·669	6·668	6·667	6·666	6·676	6·666
0·15	5·247	5·237	5·230	5·225	5·237	5·228
0·20	4·355	4·341	4·331	4·326	4·338	4·329
0·30	3·212	3·198	3·188	3·183	3·192	3·186
0·40	2·456	2·444	2·437	2·433	2·440	2·435
0·50	1·890	1·882	1·878	1·875	1·878	1·877
0·60	1·439	1·433	1·431	1·430	1·430	1·431
0·70	1·065	1·061	1·060	1·060	1·058	1·060
0·80	0·746	0·741	0·740	0·740	0·737	0·740
0·90	0·453	0·448	0·445	0·446	0·443	0·445
0·95	0·298	0·292	0·290	0·290	0·288	0·290

X	$\Delta C_p/\alpha$ at $\eta = 0{\cdot}9239$					
	NPL method			NLR method		
	$q = 4$	$q = 6$	$q = 8$	$q = 4$	$q = 6$	$q = 8$
0·0050	28·768	28·798	28·802	28·804	28·812	28·803
0·0125	17·781	17·798	17·799	17·801	17·806	17·800
0·0250	12·098	12·106	12·107	12·110	12·114	12·109
0·05	7·912	7·915	7·915	7·915	7·918	7·915
0·10	4·769	4·766	4·766	4·765	4·769	4·765
0·15	3·303	3·298	3·298	3·297	3·300	3·297
0·20	2·415	2·410	2·409	2·408	2·411	2·409
0·30	1·388	1·384	1·383	1·382	1·384	1·383
0·40	0·837	0·834	0·833	0·833	0·834	0·833
0·50	0·522	0·520	0·520	0·520	0·520	0·520
0·60	0·337	0·337	0·336	0·337	0·336	0·336
0·70	0·227	0·227	0·227	0·228	0·227	0·227
0·80	0·157	0·157	0·157	0·158	0·157	0·157
0·90	0·102	0·101	0·101	0·101	0·101	0·101
0·95	0·070	0·069	0·069	0·070	0·069	0·069

TABLE 7

Convergence of ΔC_p with Respect to q for the Hyperbolic Planform ($M = 0$, $m = 15$, $N = 4$)

NPL	$\eta = 0$		$\eta = 0{\cdot}3827$		$\eta = 0{\cdot}7071$		$\eta = 0{\cdot}9239$	
X	δ_3	δ_4	δ_3	δ_4	δ_3	δ_4	δ_3	δ_4
0·005	−0·170	−0·031	−0·218	0·112	0·115	0·104	0·030	0·004
0·05	−0·029	−0·004	−0·034	0·017	0·022	0·014	0·003	0·000
0·10	−0·005	+0·001	−0·004	0·002	−0·001	−0·001	−0·003	0·000
0·20	+0·008	0·004	+0·016	−0·008	−0·014	−0·010	−0·005	−0·001
0·40	0·007	0·002	0·012	−0·006	−0·012	−0·007	−0·003	−0·001
0·60	0·002	0·000	0·000	−0·004	−0·006	−0·002	0·000	−0·001
0·80	0·001	−0·001	−0·007	−0·004	−0·005	−0·001	0·000	0·000
0·90	0·003	−0·002	−0·007	−0·005	−0·005	−0·003	−0·001	0·000

NLR	$\eta = 0$		$\eta = 0{\cdot}3827$		$\eta = 0{\cdot}7071$		$\eta = 0{\cdot}9239$	
X	δ_3	δ_4	δ_3	δ_4	δ_3	δ_4	δ_3	δ_4
0·005	0·022	−0·002	−0·045	−0·026	−0·014	−0·011	0·008	−0·009
0·05	0·005	−0·001	−0·007	−0·003	+0·005	−0·010	0·003	−0·003
0·10	0·001	−0·001	0·000	0·000	0·010	−0·010	0·004	−0·004
0·20	0·000	−0·001	0·005	0·001	0·011	−0·009	0·003	−0·003
0·40	0·000	−0·001	0·008	−0·003	0·006	−0·004	0·001	−0·001
0·60	0·002	−0·001	0·008	−0·006	0·000	+0·001	−0·001	0·000
0·80	0·004	0·000	0·006	−0·004	−0·003	0·003	−0·001	0·000
0·90	0·004	0·001	0·005	−0·002	−0·003	0·003	0·000	0·000

$$\delta_3 = \left(\frac{\Delta C_p}{\alpha}\right)_{q=6} - \left(\frac{\Delta C_p}{\alpha}\right)_{q=4}, \qquad \delta_4 = \left(\frac{\Delta C_p}{\alpha}\right)_{q=8} - \left(\frac{\Delta C_p}{\alpha}\right)_{q=6}$$

TABLE 8

Convergence of ΔC_p with Respect to N for the Hyperbolic Planform ($M = 0$, $m = 15$, $\eta = 0{\cdot}3827$)

X	Values of $\Delta C_p/\alpha$								
	NPL method			NLR method			BAC method		
	$N = 2$	$N = 3$	$N = 4$	$N = 2$	$N = 3$	$N = 4$	$N = 2$	$N = 3$	$N = 4$
0·005	31·966	31·668	31·643	31·971	31·691	31·714	31·971	31·687	31·709
0·05	9·906	9·862	9·857	9·908	9·866	9·867	9·908	9·866	9·866
0·10	6·840	6·841	6·840	6·841	6·843	6·839	6·841	6·843	6·839
0·20	4·589	4·623	4·624	4·590	4·622	4·618	4·590	4·622	4·618
0·40	2·846	2·882	2·885	2·847	2·880	2·880	2·847	2·880	2·880
0·60	1·922	1·934	1·936	1·922	1·932	1·934	1·922	1·932	1·934
0·80	1·192	1·179	1·180	1·192	1·177	1·178	1·192	1·177	1·177
0·90	0·799	0·780	0·781	0·799	0·780	0·778	0·799	0·779	0·778

X	NPL method		NLR method		BAC method	
	Δ_1	Δ_2	Δ_1	Δ_2	Δ_1	Δ_2
0·005	−0·298	−0·025	−0·280	0·023	−0·284	0·022
0·05	−0·044	−0·005	−0·042	0·001	−0·042	0·000
0·10	+0·001	−0·001	+0·002	−0·004	+0·002	−0·004
0·20	0·034	+0·001	0·032	−0·004	0·032	−0·004
0·40	0·036	0·003	0·033	0·000	0·033	0·000
0·60	0·012	0·002	0·010	0·002	0·010	0·002
0·80	−0·013	0·001	−0·015	0·001	−0·015	0·000
0·90	−0·019	0·001	−0·019	−0·002	−0·020	−0·001

$$\Delta_1 = \left(\frac{\Delta C_p}{\alpha}\right)_{N=3} - \left(\frac{\Delta C_p}{\alpha}\right)_{N=2}, \qquad \Delta_2 = \left(\frac{\Delta C_p}{\alpha}\right)_{N=4} - \left(\frac{\Delta C_p}{\alpha}\right)_{N=3}$$

TABLE 9

Convergence of ΔC_p with Respect to m for the Hyperbolic Planform
($M = 0, \eta = 0{\cdot}3827$)

X	$\Delta C_p/\alpha$ by BAC method ($N = 4$)		
	$m = 9$	$m = 13$	$m = 15$
0·0050	31·839	31·726	31·709
0·0125	20·075	20·012	20·002
0·0250	14·122	14·087	14·081
0·05	9·882	9·868	9·866
0·10	6·838	6·840	6·839
0·15	5·456	5·463	5·463
0·20	4·610	4·618	4·618
0·30	3·559	3·565	3·564
0·40	2·880	2·881	2·880
0·50	2·367	2·365	2·364
0·60	1·938	1·934	1·934
0·70	1·551	1·548	1·549
0·80	1·174	1·174	1·177
0·90	0·771	0·774	0·778
0·95	0·524	0·529	0·532

X	Values of $\Delta C_p/\alpha$ by NLR method			
	$N = 3, q = 6$		$N = 4, q = 8$	
	$m = 15$	$m = 31$	$m = 15$	$m = 31$
0·005	31·691	31·685	31·714	31·709
0·05	9·866	9·866	9·867	9·866
0·10	6·843	6·843	6·839	6·839
0·15	5·467	5·467	5·463	5·463
0·20	4·622	4·622	4·618	4·618
0·30	3·566	3·566	3·564	3·564
0·40	2·880	2·880	2·880	2·880
0·50	2·362	2·362	2·364	2·364
0·60	1·932	1·932	1·934	1·934
0·70	1·547	1·547	1·549	1·549
0·80	1·177	1·177	1·178	1·177
0·90	0·780	0·779	0·778	0·778
0·95	0·534	0·534	0·533	0·532

TABLE 10

Results for the Warren 12 Planform with Rounding $x_l(0) = 0{\cdot}044s$
($M = 0$, $N = 4$, $q = 8$)

η	Values of $cC_{LL}/\bar{c}C_L$				
	NPL $m = 15$	NPL* $m = 15$	NLR $m = 15$	NLR $m = 31$	BAC $m = 15$
0	1·1789	1·1826	1·1813	1·1927	1·1834
0·1951	1·1934	1·1942	1·1931	1·1964	1·1944
0·3827	1·1572	1·1570	1·1563	1·1562	1·1570
0·5556	1·0746	1·0739	1·0735	1·0710	1·0737
0·7071	0·9484	0·9475	0·9473	0·9448	0·9473
0·8315	0·7768	0·7760	0·7757	0·7727	0·7757
0·9239	0·5529	0·5522	0·5520	0·5500	0·5520
0·9808	0·2878	0·2874	0·2872	0·2859	0·2872

η	Values of x_{ac}				
	NPL $m = 15$	NPL* $m = 15$	NLR $m = 15$	NLR $m = 31$	BAC $m = 15$
0**	0·4049	0·3999	0·4002	0·3856	0·3982
0·1951	0·2995	0·2980	0·2981	0·2913	0·2976
0·3827	0·2650	0·2647	0·2647	0·2646	0·2647
0·5556	0·2524	0·2523	0·2521	0·2510	0·2522
0·7071	0·2353	0·2353	0·2350	0·2355	0·2353
0·8315	0·2071	0·2070	0·2065	0·2058	0·2070
0·9239	0·1549	0·1550	0·1545	0·1552	0·1550
0·9808	0·0972	0·0972	0·0970	0·0968	0·0972

	Overall values				
	NPL $m = 15$	NPL* $m = 15$	NLR $m = 15$	NLR $m = 31$	BAC $m = 15$
C_L	2·7270	2·7324	2·7373	2·7576	2·7340
$-C_m$**	3·1038	3·1051	3·1074	3·1155	3·1094
X_{ac}**	1·1382	1·1364	1·1352	1·1298	1·1373
K_s	1·090	1·075	1·067	1·000	1·061
K_w	1·010	1·010	1·010	1·008	1·010

*Instead of the standard $m = 15$ NPL rounding with $x_l(0) = 0{\cdot}04401s$, this NPL solution and both NLR solutions use identical NLR roundings with $x_l(0) = 0{\cdot}04394s$. The BAC solution uses the BAC rounding with $x_l(0) = 0{\cdot}04394s$.

**The local aerodynamic centre $x_{ac}(0)$ is referred to the actual root chord without rounding, and the pitching axis is through the actual leading apex.

TABLE 10 (continued)

Results for the Warren 12 Planform with Rounding $x_l(0) = 0{\cdot}044s$
$(M = 0, N = 4, q = 8)$

X	$\Delta C_p/\alpha$ at $\eta = 0$			$\Delta C_p/\alpha$ at $\eta = 0{\cdot}3827$		
	NPL* $m = 15$	NLR $m = 15$	NLR $m = 31$	NPL* $m = 15$	NLR $m = 15$	NLR $m = 31$
0·0050	9·864	9·859	10·579	23·710	23·701	23·746
0·0125	6·467	6·465	6·945	14·976	14·971	15·009
0·0250	4·834	4·831	5·197	10·567	10·564	10·601
0·05	3·767	3·767	4·057	7·437	7·435	7·475
0·10	3·102	3·103	3·333	5·204	5·203	5·246
0·15	2·834	2·835	3·028	4·197	4·197	4·240
0·20	2·671	2·673	2·831	3·582	3·582	3·624
0·30	2·441	2·443	2·534	2·818	2·819	2·854
0·40	2·246	2·249	2·277	2·320	2·320	2·347
0·50	2·057	2·059	2·033	1·937	1·936	1·955
0·60	1·860	1·862	1·795	1·608	1·608	1·618
0·70	1·645	1·646	1·553	1·303	1·302	1·307
0·80	1·386	1·386	1·287	0·999	0·998	0·998
0·90	1·023	1·023	0·939	0·663	0·662	0·661
0·95	0·742	0·742	0·679	0·454	0·453	0·451

X	$\Delta C_p/\alpha$ at $\eta = 0{\cdot}7071$			$\Delta C_p/\alpha$ at $\eta = 0{\cdot}9239$		
	NPL* $m = 15$	NLR $m = 15$	NLR $m = 31$	NPL* $m = 15$	NLR $m = 15$	NLR $m = 31$
0·0050	30·391	30·356	30·325	33·359	33·292	33·260
0·0125	19·153	19·131	19·119	20·820	20·775	20·759
0·0250	13·461	13·445	13·446	14·395	14·355	14·350
0·05	9·398	9·386	9·398	9·715	9·683	9·686
0·10	6·462	6·454	6·477	6·217	6·188	6·200
0·15	5·114	5·107	5·135	4·552	4·525	4·541
0·20	4·278	4·271	4·301	3·501	3·476	3·495
0·30	3·221	3·215	3·245	2·185	2·165	2·186
0·40	2·527	2·521	2·547	1·384	1·369	1·389
0·50	2·003	1·997	2·018	0·866	0·856	0·873
0·60	1·574	1·568	1·582	0·535	0·529	0·541
0·70	1·203	1·197	1·205	0·338	0·334	0·341
0·80	0·866	0·861	0·863	0·232	0·230	0·231
0·90	0·538	0·534	0·531	0·173	0·172	0·168
0·95	0·355	0·352	0·349	0·135	0·134	0·130

*Instead of the standard $m = 15$ NPL rounding with $x_l(0) = 0{\cdot}04401s$, this NPL solution and both NLR solutions use identical NLR roundings with $x_l(0) = 0{\cdot}04394s$. The BAC solution uses the BAC rounding with $x_l(0) = 0{\cdot}04394s$.

TABLE 11

Convergence of ΔC_p with Respect to q for the Warren 12 Planform with Rounding $x_l(0) = 0{\cdot}044s$ ($M = 0, m = 15, N = 3$)

X	Values of $\Delta C_p/\alpha$ at $\eta = 0$							
	NPL method				NLR method			
	$q = 1$	$q = 2$	$q = 4$	$q = 6$	$q = 1$	$q = 2$	$q = 4$	$q = 6$
0·005	11·263	9·920	9·927	9·846	10·159	10·085	10·190	10·207
0·05	4·159	3·694	3·681	3·659	3·736	3·727	3·754	3·759
0·10	3·356	3·012	2·993	2·981	3·019	3·023	3·037	3·040
0·15	3·033	2·753	2·732	2·725	2·744	2·753	2·761	2·763
0·20	2·841	2·610	2·588	2·584	2·592	2·604	2·608	2·609
0·30	2·576	2·428	2·410	2·409	2·404	2·417	2·416	2·417
0·40	2·347	2·275	2·263	2·265	2·253	2·264	2·260	2·260
0·50	2·110	2·110	2·104	2·108	2·093	2·100	2·096	2·095
0·60	1·852	1·915	1·917	1·921	1·907	1·909	1·904	1·903
0·70	1·564	1·679	1·687	1·692	1·679	1·677	1·672	1·670
0·80	1·238	1·384	1·397	1·402	1·391	1·386	1·381	1·380
0·90	0·842	0·985	1·000	1·003	0·996	0·989	0·985	0·984
0·95	0·582	0·698	0·710	0·713	0·708	0·702	0·699	0·698

X	Values of $\Delta C_p/\alpha$ at $\eta = 0{\cdot}3827$							
	NPL method				NLR method			
	$q = 1$	$q = 2$	$q = 4$	$q = 6$	$q = 1$	$q = 2$	$q = 4$	$q = 6$
0·005	27·275	22·995	23·518	23·547	24·341	23·652	23·616	23·613
0·05	8·240	7·299	7·408	7·414	7·588	7·441	7·433	7·433
0·10	5·546	5·162	5·200	5·203	5·273	5·217	5·214	5·214
0·15	4·317	4·198	4·203	4·203	4·223	4·211	4·211	4·211
0·20	3·570	3·606	3·591	3·590	3·580	3·595	3·596	3·596
0·30	2·668	2·861	2·825	2·823	2·782	2·823	2·826	2·826
0·40	2·125	2·363	2·321	2·319	2·267	2·317	2·320	2·320
0·50	1·750	1·973	1·934	1·931	1·879	1·927	1·931	1·931
0·60	1·462	1·636	1·603	1·600	1·556	1·597	1·600	1·600
0·70	1·215	1·323	1·300	1·297	1·265	1·294	1·297	1·297
0·80	0·975	1·013	1·000	0·998	0·978	0·995	0·997	0·997
0·90	0·689	0·673	0·669	0·667	0·659	0·665	0·666	0·666
0·95	0·490	0·461	0·460	0·459	0·456	0·458	0·459	0·459

TABLE 11 (continued)

Convergence of ΔC_p with Respect to q for the Warren 12 Planform with Rounding $x_l(0) = 0{\cdot}044s$ ($M = 0, m = 15, N = 3$)

X	Values of $\Delta C_p/\alpha$ at $\eta = 0{\cdot}7071$							
	NPL method				NLR method			
	$q = 1$	$q = 2$	$q = 4$	$q = 6$	$q = 1$	$q = 2$	$q = 4$	$q = 6$
0·005	35·452	29·902	30·241	30·350	31·121	30·472	30·355	30·348
0·05	10·472	9·289	9·363	9·385	9·548	9·409	9·385	9·384
0·10	6·865	6·418	6·447	6·454	6·513	6·460	6·453	6·452
0·15	5·198	5·101	5·108	5·108	5·117	5·106	5·106	5·106
0·20	4·177	4·283	4·277	4·273	4·253	4·266	4·270	4·271
0·30	2·942	3·246	3·226	3·218	3·167	3·205	3·214	3·215
0·40	2·207	2·559	2·534	2·525	2·465	2·511	2·521	2·521
0·50	1·715	2·036	2·010	2·001	1·943	1·988	1·997	1·997
0·60	1·360	1·602	1·580	1·573	1·523	1·561	1·568	1·568
0·70	1·083	1·224	1·206	1·202	1·165	1·193	1·197	1·197
0·80	0·840	0·880	0·868	0·865	0·843	0·859	0·861	0·861
0·90	0·582	0·543	0·537	0·537	0·528	0·534	0·533	0·533
0·95	0·411	0·358	0·354	0·354	0·351	0·353	0·352	0·352

X	Values of $\Delta C_p/\alpha$ at $\eta = 0{\cdot}9239$							
	NPL method				NLR method			
	$q = 1$	$q = 2$	$q = 4$	$q = 6$	$q = 1$	$q = 2$	$q = 4$	$q = 6$
0·005	36·609	33·470	33·835	33·847	34·245	33·802	33·781	33·778
0·05	10·293	9·626	9·697	9·699	9·766	9·678	9·674	9·673
0·10	6·353	6·101	6·122	6·122	6·129	6·102	6·101	6·101
0·15	4·500	4·446	4·442	4·442	4·420	4·422	4·423	4·423
0·20	3·359	3·419	3·402	3·401	3·364	3·382	3·383	3·384
0·30	1·998	2·168	2·138	2·137	2·086	2·119	2·121	2·122
0·40	1·228	1·423	1·392	1·390	1·340	1·376	1·378	1·378
0·50	0·764	0·938	0·911	0·910	0·867	0·898	0·900	0·900
0·60	0·484	0·611	0·591	0·590	0·559	0·582	0·583	0·583
0·70	0·318	0·387	0·376	0·376	0·358	0·371	0·371	0·371
0·80	0·223	0·234	0·232	0·232	0·227	0·229	0·230	0·230
0·90	0·158	0·126	0·130	0·130	0·136	0·130	0·130	0·130
0·95	0·118	0·079	0·085	0·085	0·092	0·085	0·085	0·085

TABLE 12

Results for the Warren 12 Planform with Rounding $x_l(0) = 0{\cdot}088s$
$(M = 0, N = 4, q = 8)$

η	Values of $cC_{LL}/\bar{c}C_L$			Values of x_{ac}		
	NPL* $m = 15$	NLR $m = 15$	NLR** $m = 31$	NPL* $m = 15$	NLR $m = 15$	NLR** $m = 31$
0†	1·2007	1·2002	1·2009	0·4009	0·4009	0·3998
0·1951	1·1977	1·1974	1·1969	0·2930	0·2929	0·2930
0·3827	1·1553	1·1552	1·1554	0·2647	0·2646	0·2651
0·5556	1·0697	1·0700	1·0698	0·2516	0·2515	0·2512
0·7071	0·9430	0·9433	0·9435	0·2356	0·2352	0·2355
0·8315	0·7714	0·7716	0·7715	0·2067	0·2062	0·2059
0·9239	0·5490	0·5490	0·5491	0·1554	0·1549	0·1553
0·9808	0·2855	0·2855	0·2855	0·0968	0·0966	0·0969

	Overall values		
	NPL* $m = 15$	NLR $m = 15$	NLR** $m = 31$
C_L	2·7601	2·7634	2·7632
$-C_m$†	3·1269	3·1272	3·1266
X_{ac}†	1·1329	1·1316	1·1315

*All three solutions correspond to the NLR rounding of equation (17) with $y_i = 0{\cdot}19509s$ and $x_l(0) = 0{\cdot}08802s$.

**All the values from the NLR method with $m = 31$, $N = 4$, $q = 8$ are considered to be accurate to 3 or 4 significant figures.

†The local aerodynamic centre $x_{ac}(0)$ is referred to the actual root chord without rounding, and the pitching axis is through the actual leading apex.

TABLE 12 (continued)

Results for the Warren 12 Planform with Rounding $x_l(0) = 0{\cdot}088s$
$(M = 0, N = 4, q = 8)$

X	$\Delta C_p/\alpha$ at $\eta = 0$			$\Delta C_p/\alpha$ at $\eta = 0{\cdot}3827$		
	NPL* $m = 15$	NLR $m = 15$	NLR** $m = 31$	NPL* $m = 15$	NLR $m = 15$	NLR** $m = 31$
0·0050	13·385	13·391	13·444	23·831	23·826	23·710
0·0125	8·616	8·620	8·655	15·060	15·057	14·989
0·0250	6·265	6·268	6·294	10·633	10·631	10·590
0·05	4·660	4·663	4·683	7·493	7·492	7·472
0·10	3·581	3·583	3·600	5·254	5·254	5·250
0·15	3·119	3·121	3·134	4·243	4·243	4·246
0·20	2·838	2·840	2·851	3·625	3·625	3·632
0·30	2·472	2·474	2·480	2·853	2·853	2·863
0·40	2·203	2·205	2·206	2·347	2·346	2·356
0·50	1·967	1·969	1·967	1·956	1·955	1·963
0·60	1·741	1·742	1·736	1·621	1·620	1·625
0·70	1·506	1·506	1·497	1·311	1·310	1·312
0·80	1·240	1·240	1·229	1·003	1·002	1·003
0·90	0·892	0·892	0·882	0·665	0·665	0·664
0·95	0·638	0·638	0·630	0·455	0·455	0·454

X	$\Delta C_p/\alpha$ at $\eta = 0{\cdot}7071$			$\Delta C_p/\alpha$ at $\eta = 0{\cdot}9239$		
	NPL* $m = 15$	NLR $m = 15$	NLR** $m = 31$	NPL* $m = 15$	NLR $m = 15$	NLR** $m = 31$
0·0050	30·452	30·418	30·328	33·402	33·336	33·268
0·0125	19·196	19·175	19·122	20·851	20·805	20·764
0·0250	13·497	13·482	13·450	14·420	14·383	14·356
0·05	9·430	9·420	9·403	9·738	9·705	9·690
0·10	6·494	6·486	6·483	6·238	6·209	6·204
0·15	5·145	5·138	5·141	4·573	4·545	4·545
0·20	4·308	4·301	4·308	3·521	3·496	3·498
0·30	3·248	3·242	3·250	2·203	2·183	2·189
0·40	2·549	2·543	2·552	1·399	1·384	1·391
0·50	2·020	2·014	2·021	0·877	0·867	0·874
0·60	1·586	1·580	1·584	0·542	0·536	0·542
0·70	1·210	1·205	1·206	0·341	0·338	0·341
0·80	0·870	0·864	0·864	0·233	0·231	0·231
0·90	0·538	0·534	0·532	0·171	0·170	0·168
0·95	0·354	0·352	0·350	0·133	0·132	0·130

*NLR rounding.
**$\Delta C_p/\alpha$ is considered to be accurate to 3 or 4 significant figures.

TABLE 13

Convergence of Solutions with Respect to N for the Warren 12 Planform with Rounding $x_l(0) = 0{\cdot}088s$ ($M = 0$, $m = 15$)

η	Values of $cC_{LL}/\bar{c}C_L$			Values of x_{ac}		
	BAC method			BAC method		
	$N = 2$	$N = 3$	$N = 4$	$N = 2$	$N = 3$	$N = 4$
0†	1·1989	1·2011	1·2015	0·3953	0·3985	0·3988
0·1951	1·1984	1·1981	1·1980	0·2921	0·2923	0·2923
0·3827	1·1558	1·1553	1·1552	0·2653	0·2646	0·2646
0·5556	1·0695	1·0695	1·0695	0·2514	0·2515	0·2516
0·7071	0·9428	0·9427	0·9427	0·2356	0·2356	0·2356
0·8315	0·7721	0·7712	0·7711	0·2076	0·2068	0·2067
0·9239	0·5489	0·5483	0·5487	0·1597	0·1551	0·1554
0·9808	0·2832	0·2857	0·2853	0·1095	0·1028	0·0967

η	Values of $cC_{DL}/\bar{c}C_L^2$		
	BAC method		
	$N = 2$	$N = 3$	$N = 4$
0	0·3578	0·3660	0·3679
0·1951	0·2303	0·2452	0·2449
0·3827	0·1366	0·1440	0·1427
0·5556	0·0668	0·0790	0·0781
0·7071	0·0058	0·0213	0·0213
0·8315	−0·0469	−0·0320	−0·0214
0·9239	−0·0607	−0·0950	−0·0848
0·9808	0·0017	−0·0487	−0·0911

	Overall values		
	BAC method		
	$N = 2$	$N = 3$	$N = 4$
C_L	2·7601	2·7618	2·7621
$-C_m$†	3·1242	3·1264	3·1267
X_{ac}†	1·1319	1·1320	1·1320
K_s	0·942	0·998	1·000
K_w	1·008	1·008	1·008

†*See* footnote to Table 12.

TABLE 13 (continued)

Convergence of Solutions with Respect to N for the Warren 12 Planform with Rounding $x_l(0) = 0{\cdot}088s$ ($M = 0, m = 15$)

X	Values of $\Delta C_p/\alpha$ at $\eta = 0$			Values of $\Delta C_p/\alpha$ at $\eta = 0{\cdot}3827$		
	BAC method			BAC method		
	$N = 2$	$N = 3$	$N = 4$	$N = 2$	$N = 3$	$N = 4$
0·0050	14·479	13·783	13·629	24·099	23·801	23·852
0·0125	9·243	8·837	8·762	15·214	15·047	15·073
0·0250	6·635	6·388	6·358	10·724	10·630	10·643
0·05	4·827	4·705	4·712	7·534	7·500	7·501
0·10	3·593	3·572	3·603	5·252	5·266	5·259
0·15	3·066	3·092	3·126	4·221	4·256	4·248
0·20	2·756	2·809	2·838	3·591	3·637	3·628
0·30	2·380	2·454	2·465	2·811	2·860	2·855
0·40	2·129	2·202	2·194	2·308	2·348	2·348
0·50	1·919	1·978	1·958	1·929	1·953	1·956
0·60	1·714	1·752	1·732	1·612	1·616	1·621
0·70	1·492	1·508	1·497	1·321	1·307	1·311
0·80	1·230	1·225	1·230	1·032	1·003	1·003
0·90	0·880	0·861	0·883	0·703	0·668	0·665
0·95	0·626	0·607	0·631	0·489	0·459	0·455

X	Values of $\Delta C_p/\alpha$ at $\eta = 0{\cdot}7071$			Values of $\Delta C_p/\alpha$ at $\eta = 0{\cdot}9239$		
	BAC method			BAC method		
	$N = 2$	$N = 3$	$N = 4$	$N = 2$	$N = 3$	$N = 4$
0·0050	31·135	30·460	30·458	31·980	33·929	33·416
0·0125	19·585	19·201	19·200	19·988	21·118	20·859
0·0250	13·723	13·500	13·500	13·855	14·536	14·425
0·05	9·526	9·432	9·433	9·407	9·732	9·741
0·10	6·484	6·494	6·497	6·111	6·150	6·240
0·15	5·088	5·146	5·148	4·561	4·467	4·573
0·20	4·227	4·309	4·310	3·590	3·425	3·521
0·30	3·155	3·249	3·250	2·372	2·156	2·203
0·40	2·470	2·551	2·551	1·606	1·406	1·399
0·50	1·969	2·022	2·021	1·069	0·922	0·877
0·60	1·568	1·588	1·587	0·675	0·598	0·543
0·70	1·226	1·212	1·211	0·383	0·380	0·342
0·80	0·912	0·870	0·870	0·172	0·233	0·233
0·90	0·592	0·537	0·538	0·034	0·129	0·171
0·95	0·402	0·354	0·354	−0·005	0·083	0·133

TABLE 14

Central Chordwise Loading for the Warren 12 Planform with various roundings ($M = 0$, $m = 15$, $N = 4$)

Rounding	NPL	NLR	BAC	NLR	BAC
η_i	0·19509	0·09739	0·10388	0·19509	0·20809
$x_l(0)/s$	0·04401	0·04394	0·04394	0·08802	0·08802
X	Values of $\Delta C_p/\alpha$ at $\eta = 0$				
0·0050	9·393	9·859	10·033	13·391	13·629
0·0125	6·182	6·465	6·568	8·620	8·762
0·0250	4·647	4·831	4·899	6·268	6·358
0·05	3·653	3·767	3·804	4·663	4·712
0·10	3·044	3·103	3·117	3·583	3·603
0·15	2·802	2·835	2·840	3·121	3·126
0·20	2·655	2·673	2·673	2·840	2·838
0·30	2·442	2·443	2·438	2·474	2·465
0·40	2·256	2·249	2·242	2·205	2·194
0·50	2·072	2·059	2·052	1·969	1·958
0·60	1·880	1·862	1·855	1·742	1·732
0·70	1·668	1·646	1·638	1·506	1·497
0·80	1·411	1·386	1·378	1·240	1·230
0·90	1·047	1·023	1·015	0·892	0·883
0·95	0·762	0·742	0·735	0·638	0·631

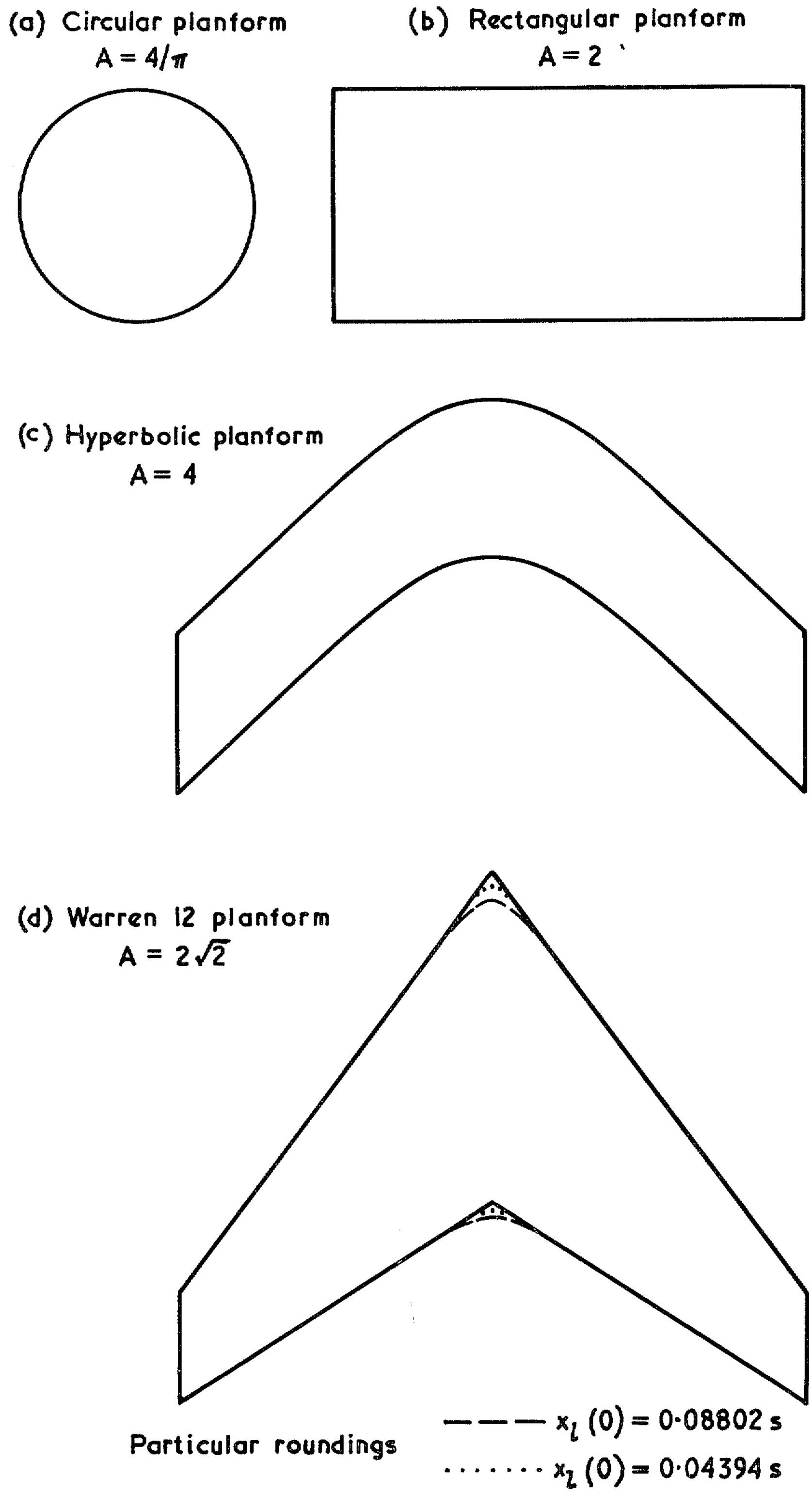

FIG. 1. Four planforms used as examples.

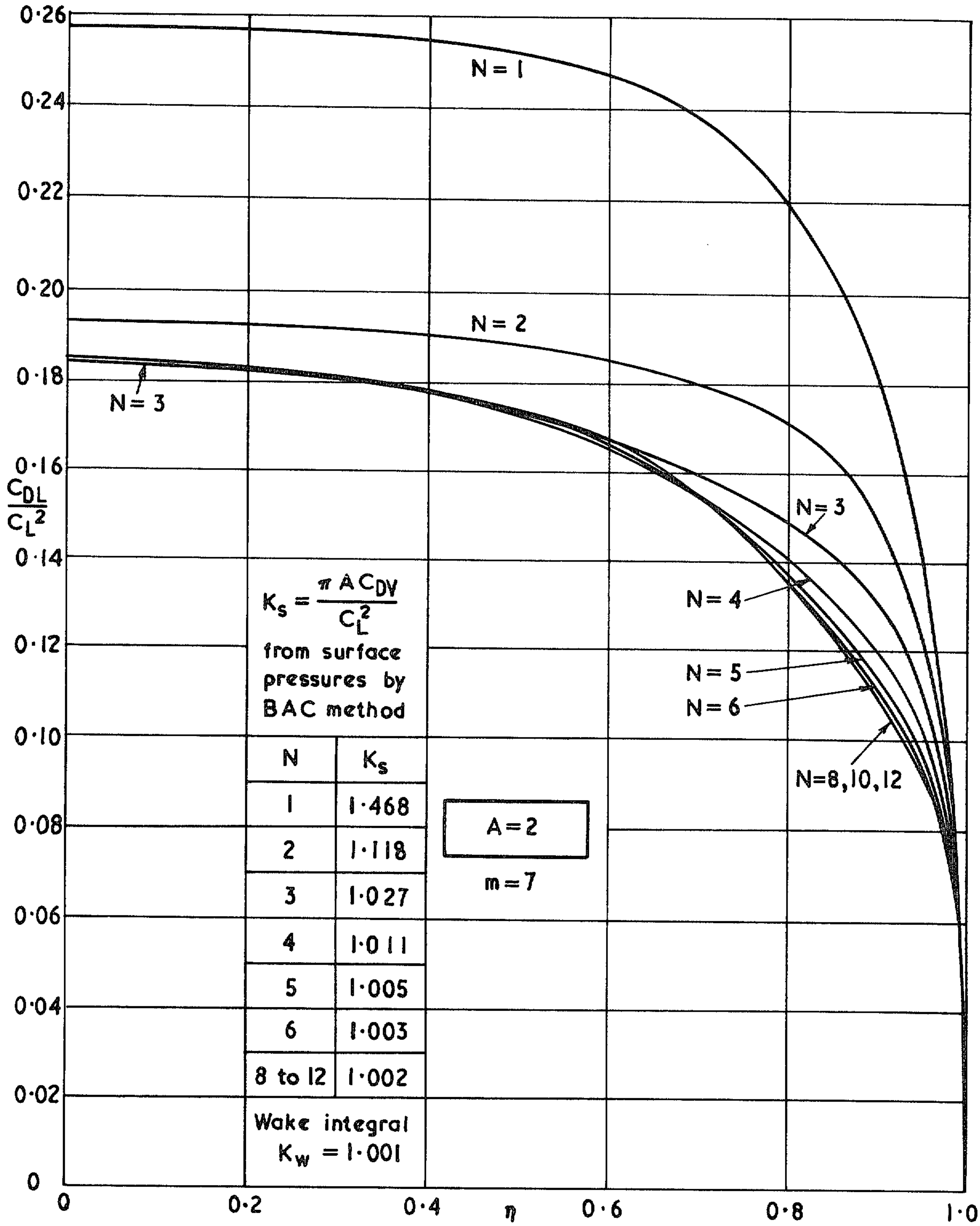

FIG. 2. Convergence of vortex-drag distribution on the rectangular wing with an increasing number of chordwise terms in the solution.

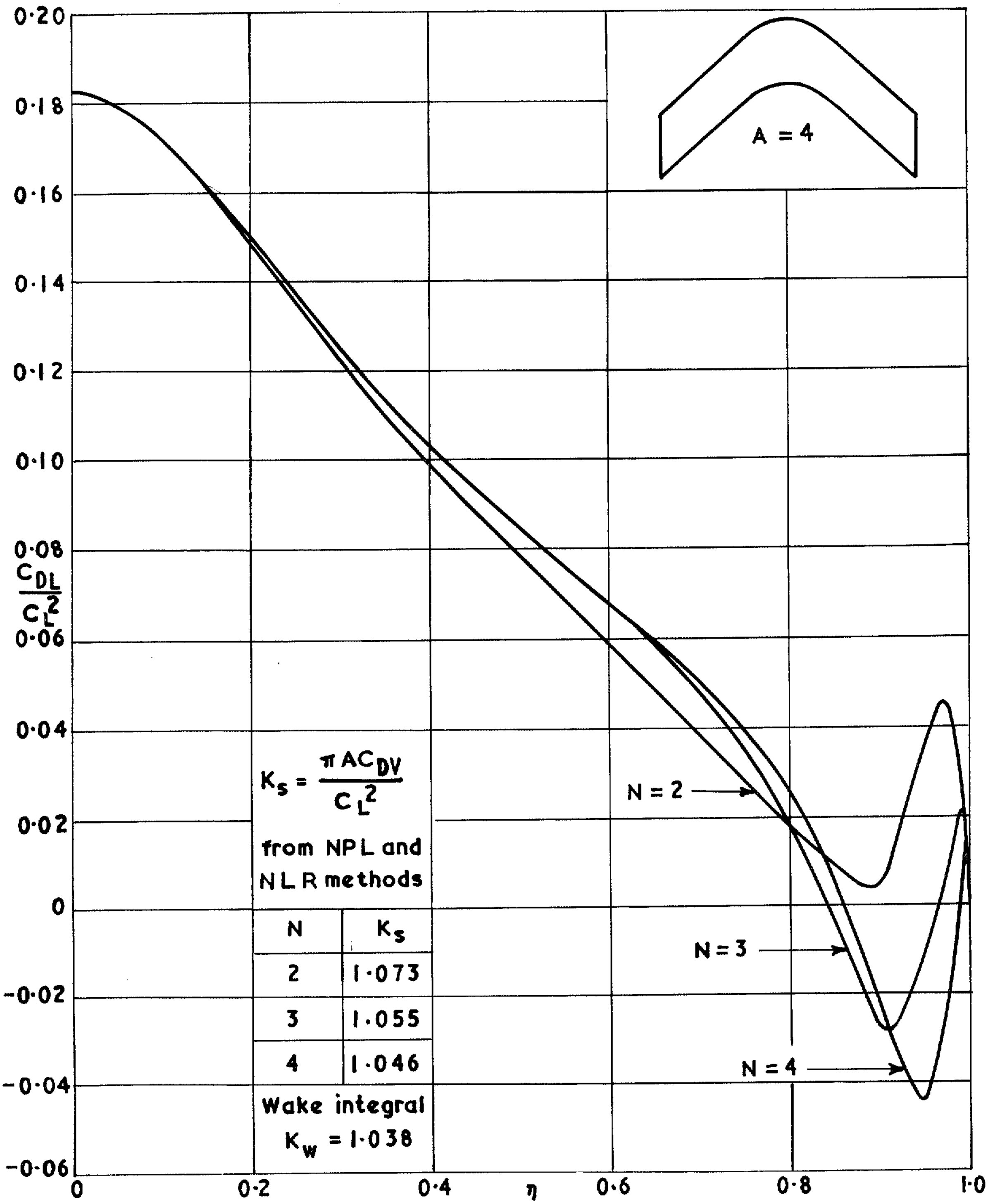

FIG. 3. Convergence of vortex-drag distribution on the hyperbolic wing with an increasing number of chordwise terms in the solution.

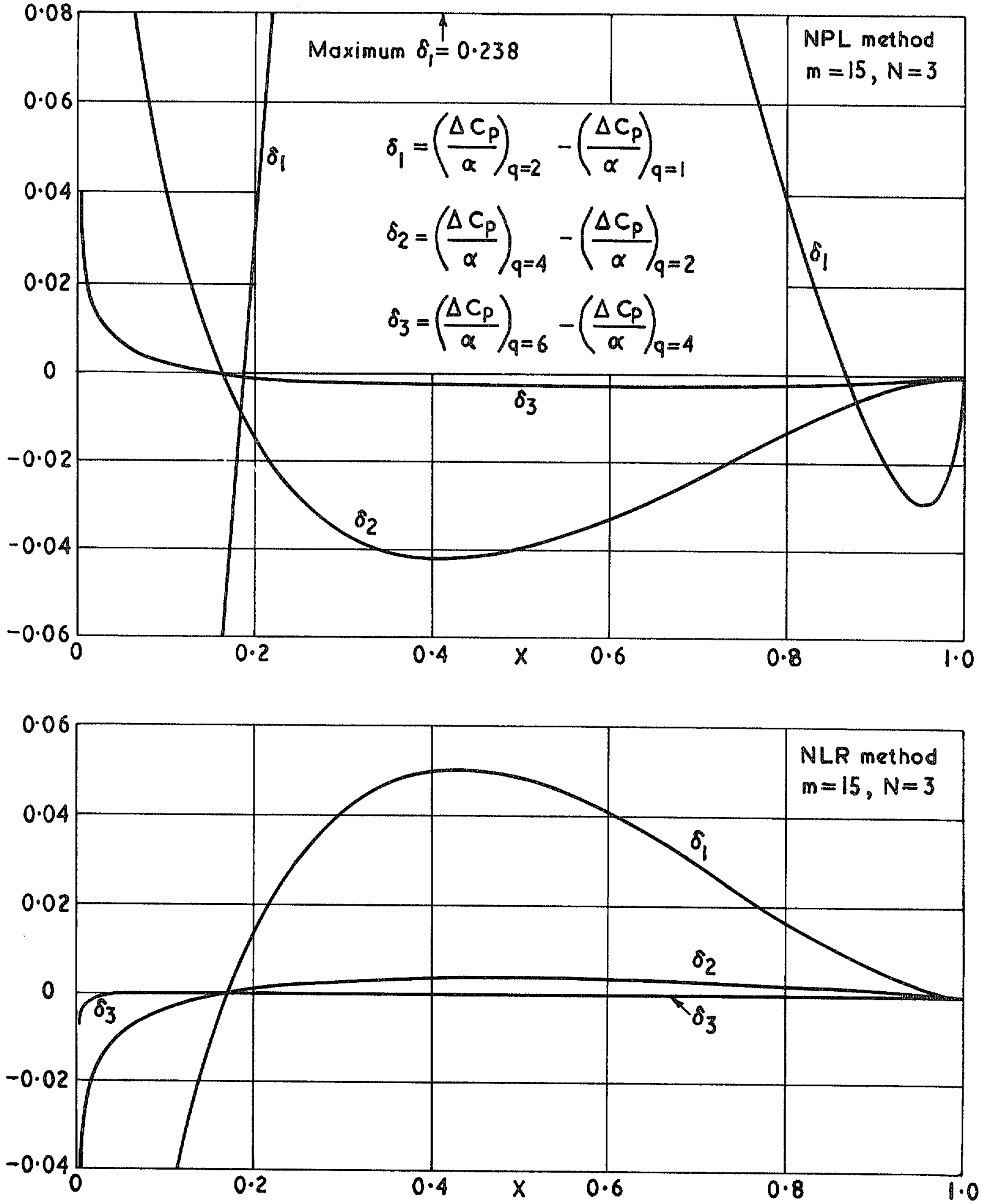

FIG. 4. Convergence of chordwise loading on Warren 12 planform with an increasing number of spanwise integration points (η = 0·3827).

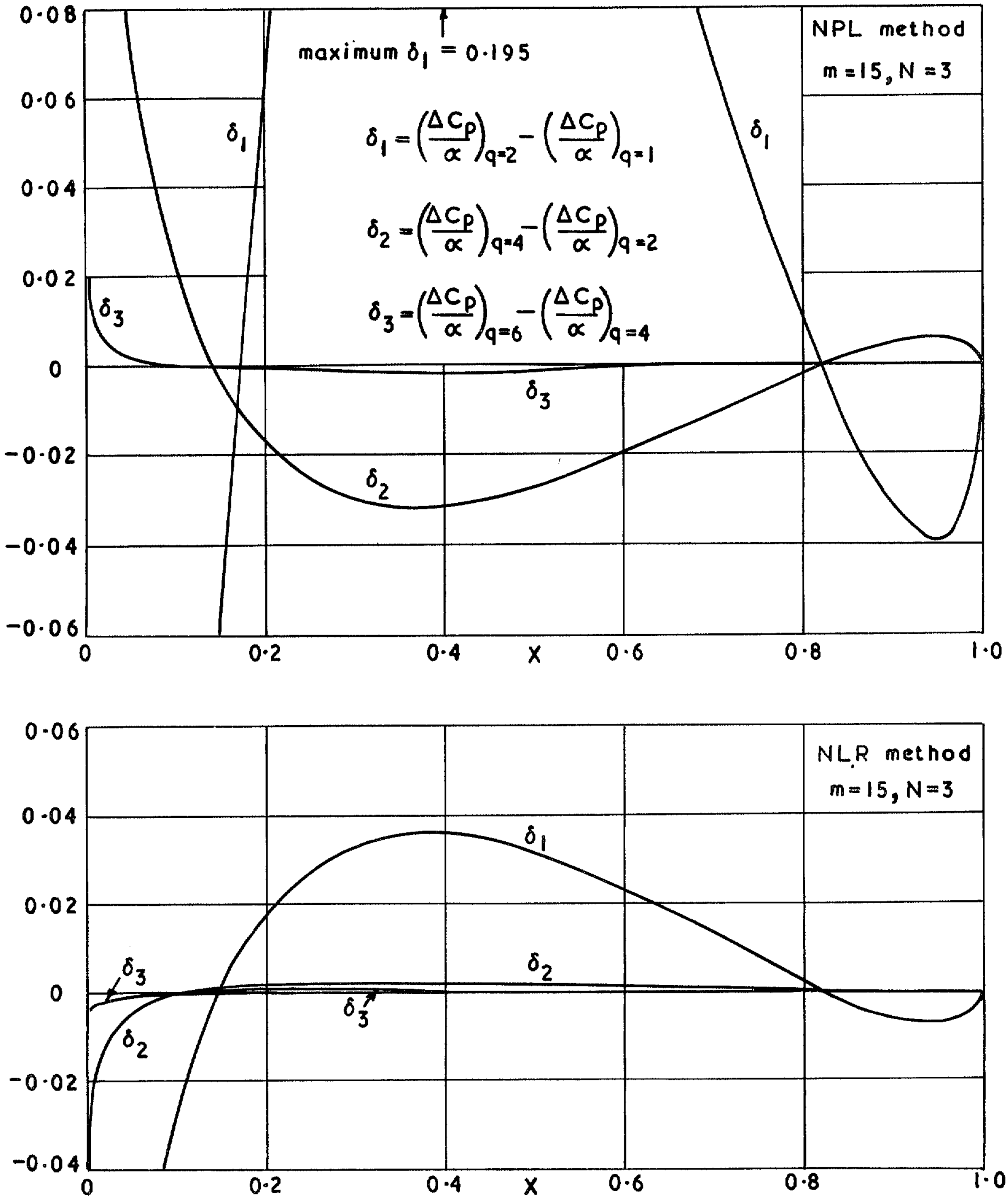

FIG. 5. Convergence of chordwise loading on Warren 12 planform with an increasing number of spanwise integration points (η = 0·9239).

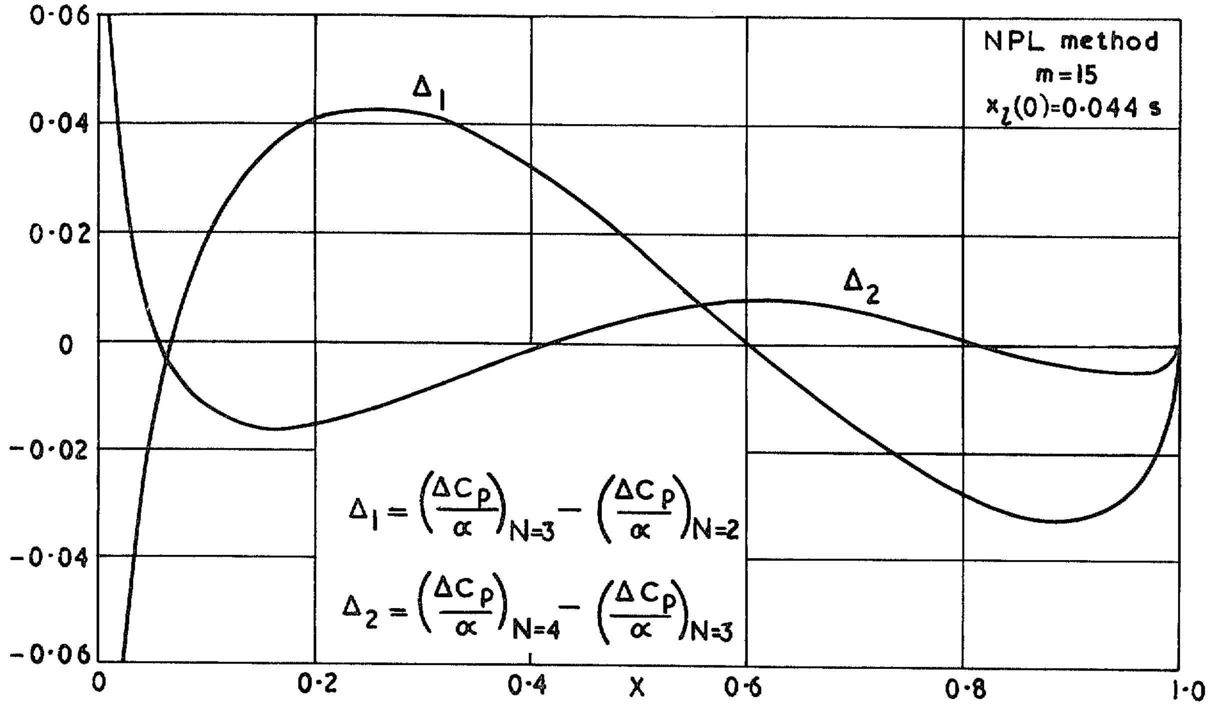

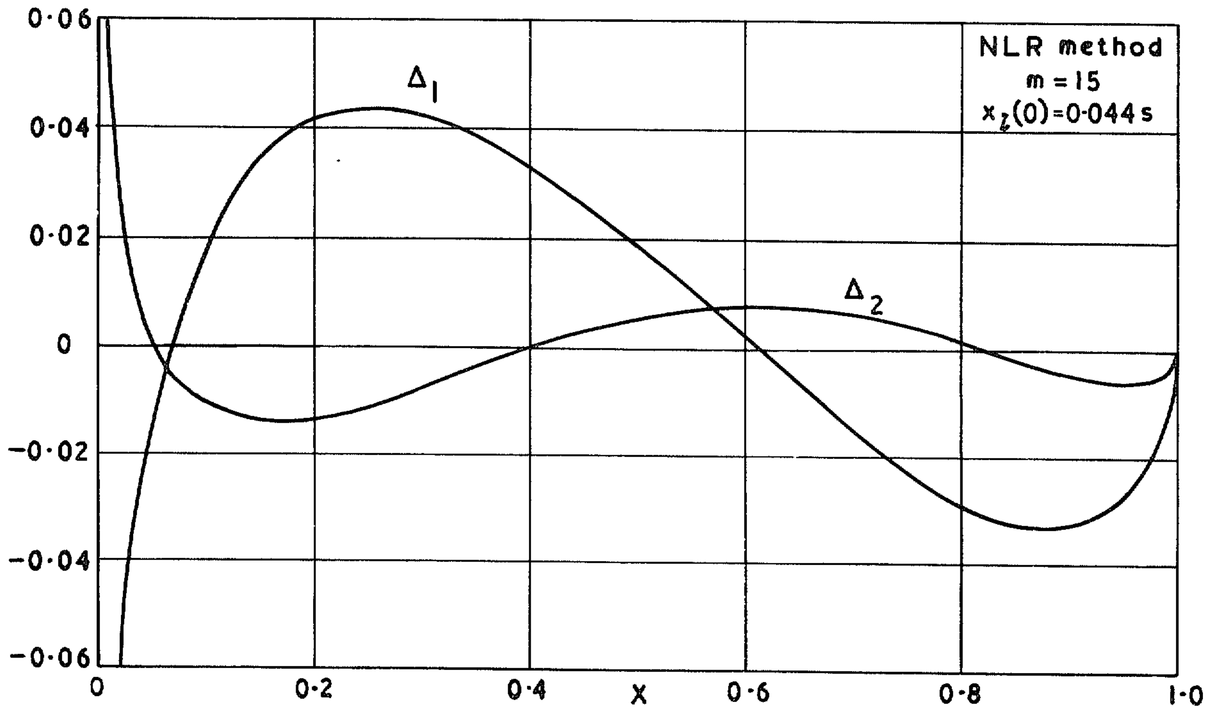

FIG. 6. Convergence of the chordwise loading on Warren 12 planform at $\eta = 0{\cdot}3827$ with an increasing number of chordwise collocation points.

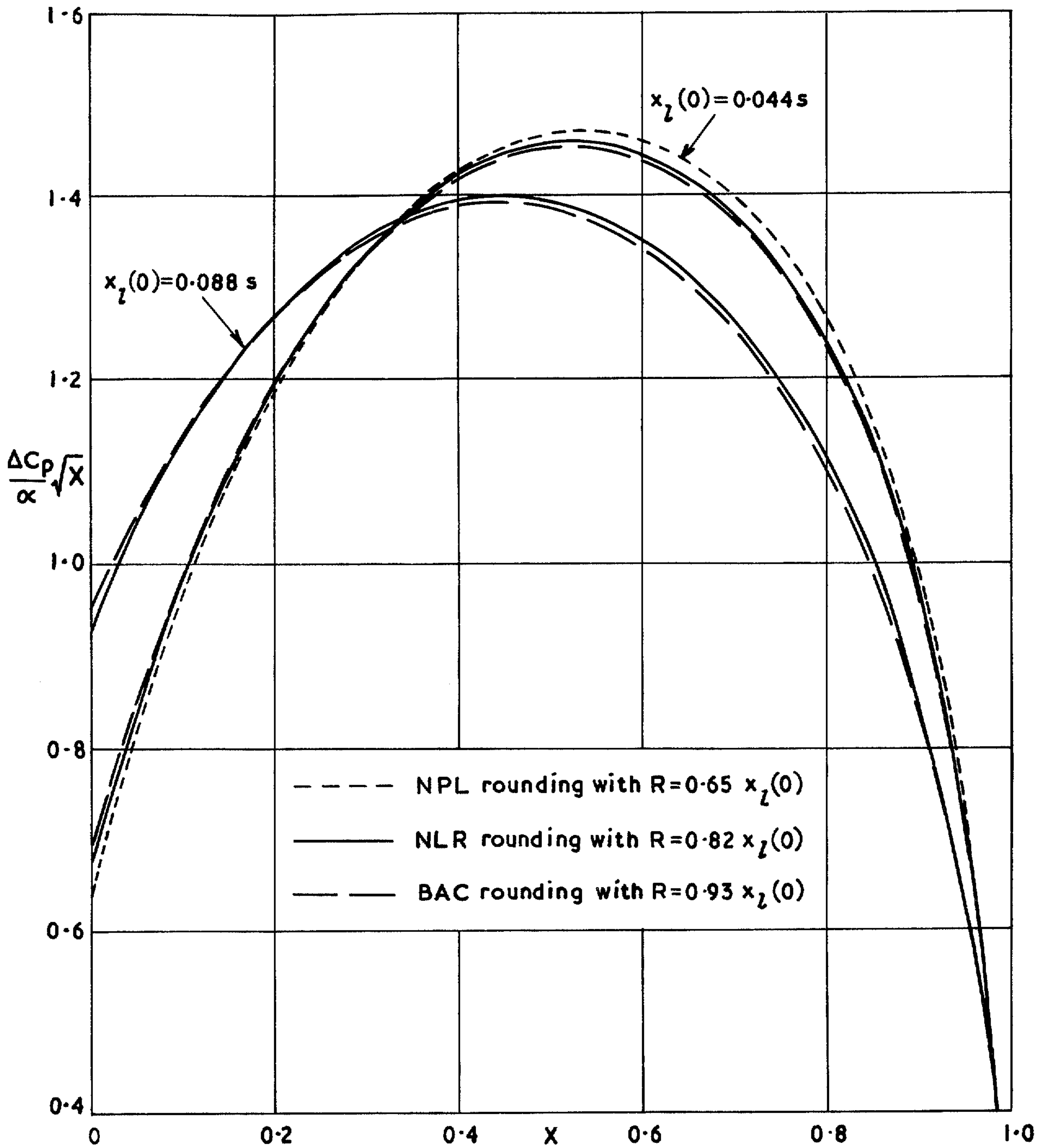

FIG 7. Effect of magnitude and type of central rounding on the chordwise loading at the centre section of the Warren 12 planform.

Printed in England for Her Majesty's Stationery Office by J. W. Arrowsmith Ltd., Bristol BS3 2NT

Dd. 146916 K.5.

R. & M. No. 3597

Published by
HER MAJESTY'S STATIONERY OFFICE

To be purchased from
49 High Holborn, London W.C.1
13A Castle Street, Edinburgh EH2 3AR
109 St. Mary Street, Cardiff CF1 1JW
Brazennose Street, Manchester M60 8AS
50 Fairfax Street, Bristol BS1 3DE
258 Broad Street, Birmingham 1
7 Linenhall Street, Belfast BT2 8AY
or through any bookseller

R. & M. No. 3597

SBN 11 470198 9